
Masters Theses

Student Theses and Dissertations

1953

The lattice constant and coefficient of expansion of chromium

Chao-Ching Weng

Follow this and additional works at: https://scholarsmine.mst.edu/masters_theses



Part of the [Metallurgy Commons](#)

Department:

Recommended Citation

Weng, Chao-Ching, "The lattice constant and coefficient of expansion of chromium" (1953). *Masters Theses*. 2608.

https://scholarsmine.mst.edu/masters_theses/2608

This thesis is brought to you by Scholars' Mine, a service of the Missouri S&T Library and Learning Resources. This work is protected by U. S. Copyright Law. Unauthorized use including reproduction for redistribution requires the permission of the copyright holder. For more information, please contact scholarsmine@mst.edu.

THE LATTICE CONSTANT AND COEFFICIENT
OF EXPANSION OF CHROMIUM

By
CHAO-CHING, WENG

A
THESIS

submitted to the faculty of the
SCHOOL OF MINES AND METALLURGY OF THE UNIVERSITY OF MISSOURI
in partial fulfillment of the work required for the
Degree of
MASTER OF SCIENCE IN METALLURGICAL ENGINEERING
Rolla, Missouri
1953

Approved by


Research Professor of Metallurgy

82677

ACKNOWLEDGEMENT

The author wishes to thank the Research Corporation for their Cottrell Grant of a Graduate Fellowship, and the Missouri School of Mines and Metallurgy, Rolla, Missouri, for providing the opportunities and facilities to carry out this investigation.

The author also wishes to express his very sincere appreciation to Dr. M. E. Straumanis, Research Professor of the Department of Metallurgical Engineering, for his valuable suggestions, guidance and advice throughout this project.

Sincere thanks are also due to Dr. Robert Gilbert, of the Battelle Memorial Institute, for supplying the two purest chromium samples, and their chemical analyses, which were necessary for the undertaking of this work.

CONTENTS

	Page
Acknowledgements	11
List of Figures	v
List of Tables	vii
INTRODUCTION	1
REVIEW OF LITERATURE	3
SAMPLES USED IN THIS INVESTIGATION	6
PREPARATION OF THE SAMPLES USED FOR X-RAY DIFFRACTION	8
1. Grinding and Sieving	8
2. Evacuation and Heat Treatment	9
3. The Powder Mount	10
EQUIPMENT USED FOR X-RAY DIFFRACTION	14
1. The X-ray Camera	14
2. X-ray Machine and Temperature Control System	17
3. Comparator	24
INDEXING AND MEASURING THE FILM	26
1. Theory	26
2. Indexing the Film and Selection of the Target	28
3. Measurement of the Film	35
EXPERIMENTAL RESULTS	39
1. Lattice Constant	39
2. Coefficient of Expansion	49
3. Correction of Refraction and the Precise Lattice Constants	53

	Page
DISCUSSION	57
1. Correction of Absorption	57
2. Calculation of Atomic Weight	57
3. Calculation of X-ray Density	60
SUMMARY	61
APPENDIX	63
BIBLIOGRAPHY	73
VITA	74

LIST OF FIGURES

Figure		Page
1.	The Curves of Linear Thermal Expansion of Chromium as Obtained by Different Investigators	4
2.	A Sketch of an Evacuated and Sealed Quartz Glass Bulb with Chromium Powder Inside . . .	8
3.	Vacuum Pump Used for Evacuating the Silica Glass Bulb	9
4.	The Schematic Arrangement of the Heat Treatment System	10
5.	Set-up for Mounting, Centering and Coating of the Glass Hair	12
6.	Powder Mount 0.12 mm. in Diameter	13
7.	View of the Outside of the Precise Camera . . .	15
8.	The Precision Camera	16
9.	The Camera Locked in a Metallic Jig for Fixing in the Thermostatic Jacket	19
10.	The Camera Placed in the Thermostatic Jacket with Door Removed	20
11.	A View of the Thermostatic Jacket with the Door Closed	21
12.	The Arrangement of the Complete X-ray Diffraction Unit	23
13.	The Comparator	25
14.	The Film Arrangement in the Asymmetric Method	27
15.	Path of the X-ray Beam in a Debye-Scherrer Camera	29
16.	The Graphic Method for Indexing Film and Selecting Radiation	31
17.	Schematic Diagram of a Simplified Asymmetric Powder Pattern	35
18.	X-ray Powder Photograph of Chromium Sample with Chromium Radiation	37

Figure	Page
19. Lattice Constant of Electrolytic Chromium at Different Temperatures	45
20. Lattice Constant of Sintered Electrolytic Chromium at Different Temperatures	46
21. Lattice Constant of Iodide Chromium (Low Metallic) at Different Temperatures	47
22. Lattice Constant of Iodide Chromium (Low Non-Metallic) at Different Temperatures	48
23. Changes of Lattice Constants against Glancing Angle due to Absorption	58

LIST OF TABLES

Table		Page
I.	Figures of Lattice Constant of Chromium Obtained by Different Investigators	5
II.	Compositions of the Four Different High Purity Chromium Samples	7
III.	Values of the Diffraction Lines (Cr Radiation).	33
IV.	Mathematical Indexing Method of Pure Chromium (Cr Radiation)	34
V.	Record of Film Measurement and Calculation of Pure Chromium (Cr Radiation)	38
VI.	Lattice Constants of Electrolytic Chromium at Different Temperatures	40
VII.	Lattice Constants of Sintered Electrolytic Chromium at Different Temperatures	41
VIII.	Lattice Constants of Iodide Chromium Low in Metallic Impurities at Different Temperatures	42
IX.	Lattice Constants of Iodide Chromium Low in Non-Metallic Impurities at Different Temperatures	43
X.	Lattice Constants of Four Chromium Samples at Different Temperatures	44
XI.	Coefficient of Thermal Expansion of Electrolytic Chromium Between 13° and 50° C .	50
XII.	Coefficient of Thermal Expansion of Sintered Electrolytic Chromium Between 10° and 50° C .	51
XIII.	Coefficient of Thermal Expansion of Iodide Chromium (Low Metallic) Between 12° and 50° C	51
XIV.	Coefficient of Thermal Expansion of Iodide Chromium (Low Non-Metallic) Between 13° and 50° C	52
XV.	Coefficient of Thermal Expansion of Four Different Kinds of Chromium Samples Between 10° and 50° C	52

Table	Page
XVI. The Precise Lattice Constants of Four Different Chromium Samples	56

INTRODUCTION

The most important use of chromium, other than as an alloying element in the manufacture of stainless steel, is for electroplating; to form a coating on other metals for corrosion prevention in order to procure longer life, and to achieve a decorative effect.

The physical properties of chromium are important in the effectiveness of its uses, and its lattice constant, as well as coefficient of thermal expansion, seem worthy of exact determination.

A number of research workers, over a span of thirty years, have spent considerable effort in determining the aforementioned constants. However, their results do not check, and the degree of accuracy differs from person to person.

Chromium near 37° C was identified by M. E. Fine⁽¹⁾ as showing discontinuous changes of coefficient of expansion, Young's modulus, internal friction, electrical resistivity and thermoelectric power. Although the X-ray diffraction pattern gave no clue, a difference in the thermal expansivity has been found. D. MacNair⁽²⁾ determined the expansivity of chromium by means of an interferometric dilatometer, with the result that near 38° C the thermal expansivity curve

(1) Fine, M. E., J. of Metals Tran. A.I.M.E., p.189, 56, 1951.

(2) MacNair, D., Rev. of Scientific Instruments, p. 12, 66, 1941.

went through an inflection point, corresponding to a minimum in the coefficient of expansion found by Fine.

The purpose of this research is to check the results obtained by MacNair and Fine concerning the expansion of chromium, and to determine the exact lattice constant and thermal expansion of this metal by the X-ray powder method, using different samples, and at different temperatures within the range of 10° to 50° C.

REVIEW OF LITERATURE

After the discovery of X-ray diffraction by crystal by M. von Laue,⁽³⁾ Friedrich, and Knipping in 1912, the lattice constant of chromium could be easily determined. However, the degree of accuracy is dependent upon the purity of the sample, the method applied, and the kind of camera used.

Hull⁽⁴⁾ used a molybdenum target to produce X-rays and to investigate the lattice constant of chromium. He got a figure of 2.91 kX in 1919. In 1928, A. Westgren⁽⁵⁾ used a chromium target, and got a figure of 2.878 kX for the lattice constant. The results obtained by other investigators are shown in Table 1.

Disch⁽⁶⁾ was the first investigator to publish data in 1921 concerning the linear thermal expansion of chromium. During the next year, Chevenard⁽⁷⁾ published data on the linear thermal expansion of 98.3 percent pure chromium. Hidnert⁽⁸⁾ published data on the linear thermal expansion

(3) Laue, M., Ann. Physik, p. 41, 971, 1913 reprinted from an earlier publication in 1912.

(4) Hull, A. W., Phys. Rev. p. 14, 540, 1919.

(5) Westgren, A., J. Iron & Steel Institute, p. 117, 383, 1928.

(6) Disch, J., Z. Physik, p. 5, 173, 1921.

(7) Chevenard, P., Comptes rend. p. 174, 109, 1922.

(8) Hidnert, P., J. of Research of the National Bureau of Standards, p. 26, 81, 1941.

coefficient of 99.3 percent and 98.7 percent pure electrolytic chromium in the years of 1931 and 1934. These curves are shown in Fig. 1.

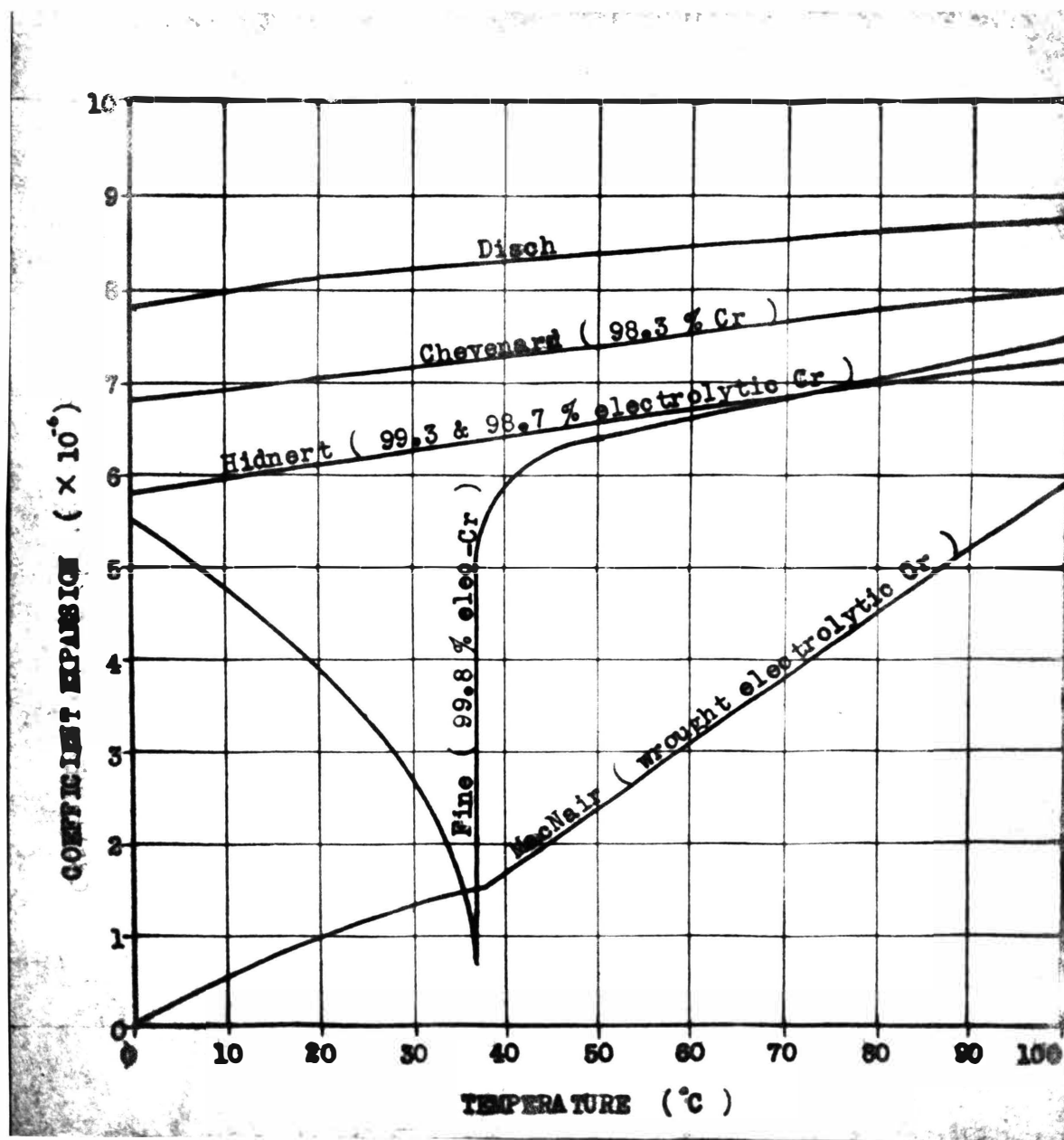


Figure 1. The curves of linear thermal expansion of chromium as obtained by different investigators.

TABLE 1
 Figures of Lattice Constant of Cr Obtained by Different Investigators

Name of research workers	Name of periodicals	Target	Temp.	Lattice Constant(kX)
A. W. Hull	Phys.Rev. p.14, 540, 1919	Mo.	room	2.91
A. W. Hull	Phys.Rev. p.17, 571, 1921	Mo.	room	2.895
Wm. C. Phebus & F.C.Blake	Phys.Rev. p.25, 107, 1925	Mo.	room	2.875
Wm. C. Phebus & F.C.Blake	Phys.Rev. p.25, 581, 1925	Mo.	room	2.873
R. A. Patterson	Phys.Rev. p. 26, 56, 1925	Mo.	room	2.872
Cyril S. Smith	Metal Ind. p.28, 456, 1926	Mo.	room	2.860
Frederick Sillers	Am.Electrochem.Soc.Trans., p.52, 301, 1927	Mo.	room	2.872 \pm 0.005
A. Westgran, G. Phragmen, & Tr. Negresco	J. Iron & Steel Institute, p.117, 383, 1928	Cr.	room	2.878
Kumazo Sasaki & Sinkiti Sekito	Am. Electrochem. Soc. Trans., p.59, 439, 1931	Cr.	room	2.877 \pm 0.003
G. D. Preston	J. Iron & Steel Institute, p.124, 139, 1931	Cr.	room	2.8786 \pm 0.0005
E. R. Jette	A. I. M. M. E. Tech, 522, 1934	Cr.	room	2.8787
L. Wright, H. Hirst, & J. Riley	Farad. Soc. Trans., p.31, 1253, 1935	Cr.	room	2.8788 2.8781
W. A. Wood	Phil. Mag., p.23, 984, 1937	Cr.	18°C	2.8796
H. Sochtig	Ann. Phys., p.38, 97, 1940	Cr.	room	2.846
M. E. Fine, E. S. Greiner . . & W. C. Ellis	J. Metals A. I. M. E. Trans, p. 189, 56, 1951	Cr.	20°C	2.87900 \pm (2.8848 Å)

SAMPLES USED IN THIS INVESTIGATION

Four high purity chromium samples were used in this investigation. Two of them were produced by electrolytic methods, and the other two by the iodide method. The iodide chromium samples (Battelle Memorial Institute) consisted of shiny crystals and were of two compositions: one sample being very low in metallics, and the other low in non-metallics such as H_2 , N_2 , C, and S. The chemical analyses, as given by the manufacturers, differ somewhat from sample to sample, and are listed in Table II.

TABLE II

Compositions of the Four Different High Purity
Chromium Samples

Impurity	Electrolytic	Sintered Electrolytic	Iodide (low metallic)	Iodide (low non-metallic)
H ₂		0.0001	0.0009	0.0001
O ₂		0.0088	0.014	0.001
N ₂		0.019	0.013	0.001
C		0.005		0.001
S				0.003
Sb		0.01		
Si			< 0.001	0.001
Fe			< 0.001	0.005 - 0.1
Cu			< 0.001	< 0.001
Mn			N. D. (1) < 0.001	0.001 - 0.01
Mg			< 0.001	< 0.001 Trace
Co			< 0.001	N. D.
Ni			N. D.	< 0.005
Ti			N. D.	N. D.
Pb			N. D.	N. D.
Ca			< 0.001	< 0.001 Trace
Al			N. D. < 0.001	0.0001-0.001
W			N. D. < 0.1 (2)	0.001 - 0.01
Mo			N. D.	N. D.
Manu- facturer:	Charles Hardy, Inc.	Niagara Falls	Battelle Memorial Institute	Battelle Memorial Institute

(1). N. D. means not detected.

(2). Tungsten probably not present but standard used was only
this sensitive.

PREPARATION OF THE SAMPLES USED FOR X-RAY DIFFRACTION

1. Grinding and Sieving

The purpose of using fine powder mounts in X-ray diffraction is to obtain sharp, uniform, and unshifted diffraction lines on the films. Such lines are necessary for the exact determination of lattice constants. For this reason, the first step in the preparation of a sample was to grind it as fine as possible with a mortar and pestle, and then sieve it. Because of plastic deformation, the metal, after grinding for several hours, was in the form of leaflets. The powder was then sieved through a 325 mesh screen, shaking the screen only slightly. Only the fine powder that passed through the sieve was filled into a silica glass bulb (Fig. 2) to be heat treated.

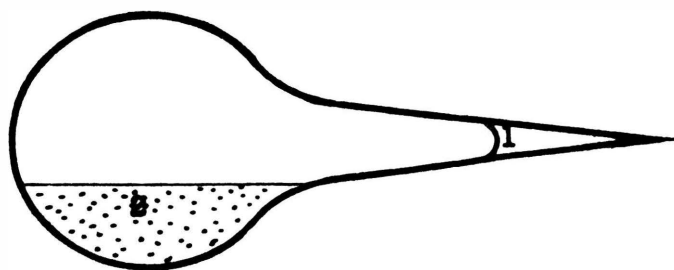


Figure 2. A sketch of an evacuated and sealed quartz glass bulb with Cr. powder inside.

(1). Sealed part; (2). Sample

2. Evacuation and Heat-treatment

The purpose of heat treatment is to get rid of hydrogen gas dissolved in the metal, and to release strains and deformation caused by grinding. However, the temperature should not be too high, as excessive grain growth, resulting from recrystallization, should be prevented. As chromium oxidizes quickly in the air at elevated temperatures, and changes its physical properties, the heating must be made in a vacuum. This can be done by connecting the silica glass bulb containing the chromium powder with a mechanical vacuum pump, which produces a vacuum as low as 1 micron of Hg. (Fig. 3) To remove the major part of the gases absorbed, the sample was heated during evacuation. After the best

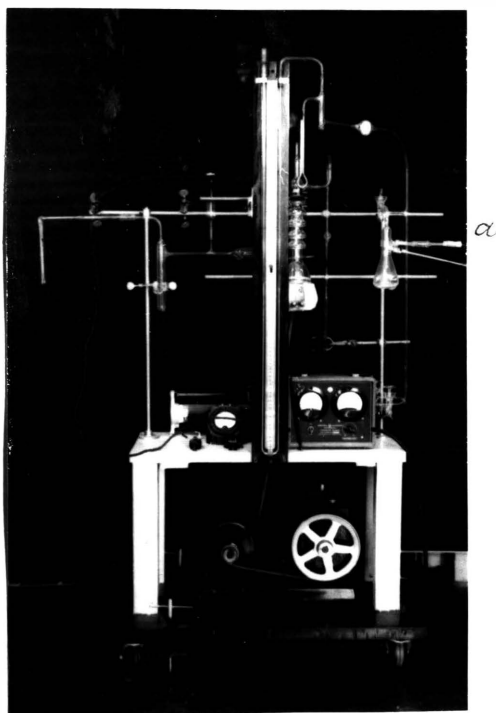


Figure 3. Vacuum pump used for evacuating the silica glass bulb (a).

vacuum obtainable was reached, the silica glass bulb was sealed off with an oxygen-gas flame. The sealed part of the bulb was examined under a microscope to be sure that no leaks were in the sealed part. The bulb with the sample inside was then transferred to the furnace for heat treatment.

The electric tube-furnace had Ni-Cr wire windings, and the temperature in the center of the furnace was measured by a chromel-alumel thermocouple and recorded automatically by a Brown potentiometer. The heating temperature in this experiment was 850° C, and the samples were held for two and a half hours at this temperature. The arrangement for the heating of the samples is shown in Figure 4.

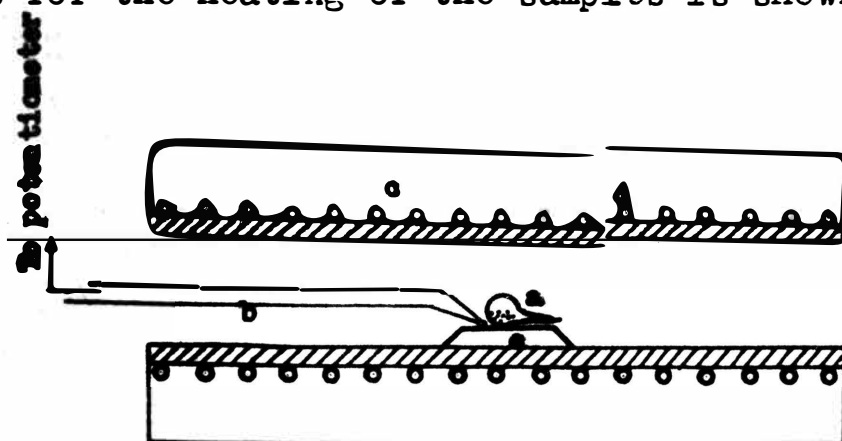


Figure 4. The schematic arrangement of the heat treatment system.

- (a). Sealed glass bulb containing sample;
- (b). Thermocouple; (c). Electric tube furnace;
- (d). Ni-Cr wire winding; (e). Porcelain boat.

3. The Powder Mount

At a temperature of 850° C, the grains of the fine chromium powder did not stick together, which was a conven-

lence in making the powder mounts to obtain X-ray diffraction patterns. For the preparation of the mounts, a thin lithium-boron glass hair was used, the constituents of the glass being 1.4 parts by weight of BeCO_3 , 4.3 parts by weight of Li_2CO_3 and 18.3 parts by weight of $\text{B}(\text{OH})_3$. The diameter of the glass hair was 0.08 mm, and its length about 10 mm. One end of the glass hair was placed in the groove at the tip of the adjustable sample holder, while the other end was supported by a cork, so that the hair was approximately parallel to the length of the groove. A drop of liquid glue (Dekadhese plastic cement) was then spread over the groove holding one end of the glass hair, and allowed to dry for 20 minutes. After that, the glass hair was cut with scissors to 5-6 mm. in length. The glass hair then held its position firmly, even when heated above 70°C . After mounting, the glass hair must be carefully centered. Both mounting and centering were done under a microscope which must have a cross hair on its objective lens (Fig. 5). Centering was achieved by adjusting the screws of the sample holder until the axis of the glass hair exactly coincided with the axis of rotation of the holder. After centering, the tip of the glass hair, about 2 mm. in length, was coated, by means of a soft copper wire of 0.1 mm. in diameter, with a small amount of non-drying glue (stop grease cello-seal diluted with oil). The layer of glue has to be thin and uniform. The tip of the hair carrying the glue was then dipped into the chromium powders,

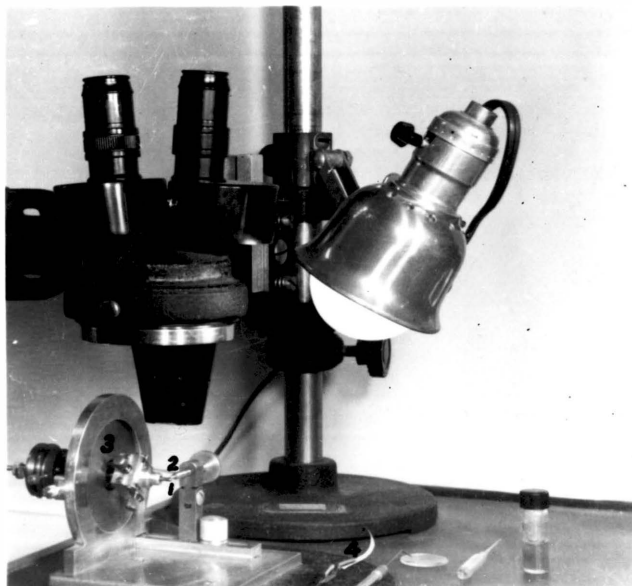


Figure 5. (1). Set up for mounting, centering and coating of the glass hair 0.08 mm. in diameter; (2). Long screw for adjusting the tip of the specimen holder; (3). Camera cover in the frame; (4). Aluminum foil for coating the glass hair with powder.

which was on the end of a thin triangle-shaped piece of aluminum foil. The fine powder adhered tightly to the glass hair especially after being rotated in the powder. The diameter of the whole sample, including the glass hair, was about 0.12 to 0.2 mm. (Fig. 6) The glass hair holding the powder rotates with the camera holder in the camera during the time of exposure by X-rays. It is important to get a thin, uniform, and well centered powder mount, because this reduces the width of the X-ray diffraction lines and their positions can be measured more accurately.

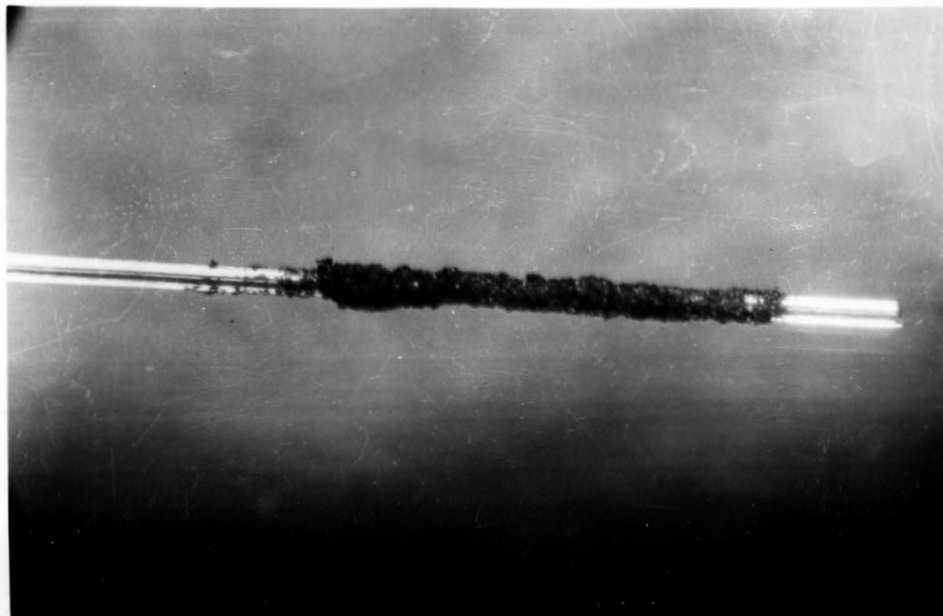


Figure 6. Powder mount 0.12 mm. in diameter.

EQUIPMENT USED FOR X-RAY DIFFRACTION

1. The X-ray Camera

The precision camera used is shown in Fig. 7 and 8. It was of a cylindrical type with a diameter of 64 mm. X-ray films of a size 3 x 18 cm. were used in this camera. The films were located in the asymmetric manner which has the following advantages:

- (1). Both, all front and back diffraction lines, are simultaneously recorded on one film.
- (2). The effective circumference of the film can be calculated from each film independently after its measurement. Thus errors due to incorrect knowledge of the diameter of the camera, and due to film shrinkage, are eliminated.
- (3). No standard substances are necessary for camera calibration.
- (4). The method is, therefore, absolute, as the absolute value of the lattice constants can be determined from the films themselves.
- (5). Further, because of the careful construction of the camera and because of the very thin sample, the error due to eccentricity is largely minimized.
- (6). The error due to absorption of X-rays is greatly reduced, especially in the high back reflection region (75° - 90°) where the shift of the lines

due to absorption can be entirely neglected.

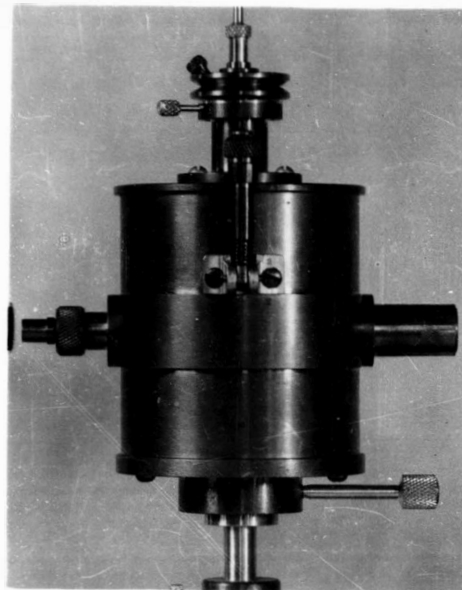


Figure 7. View of the outside of the precise camera.

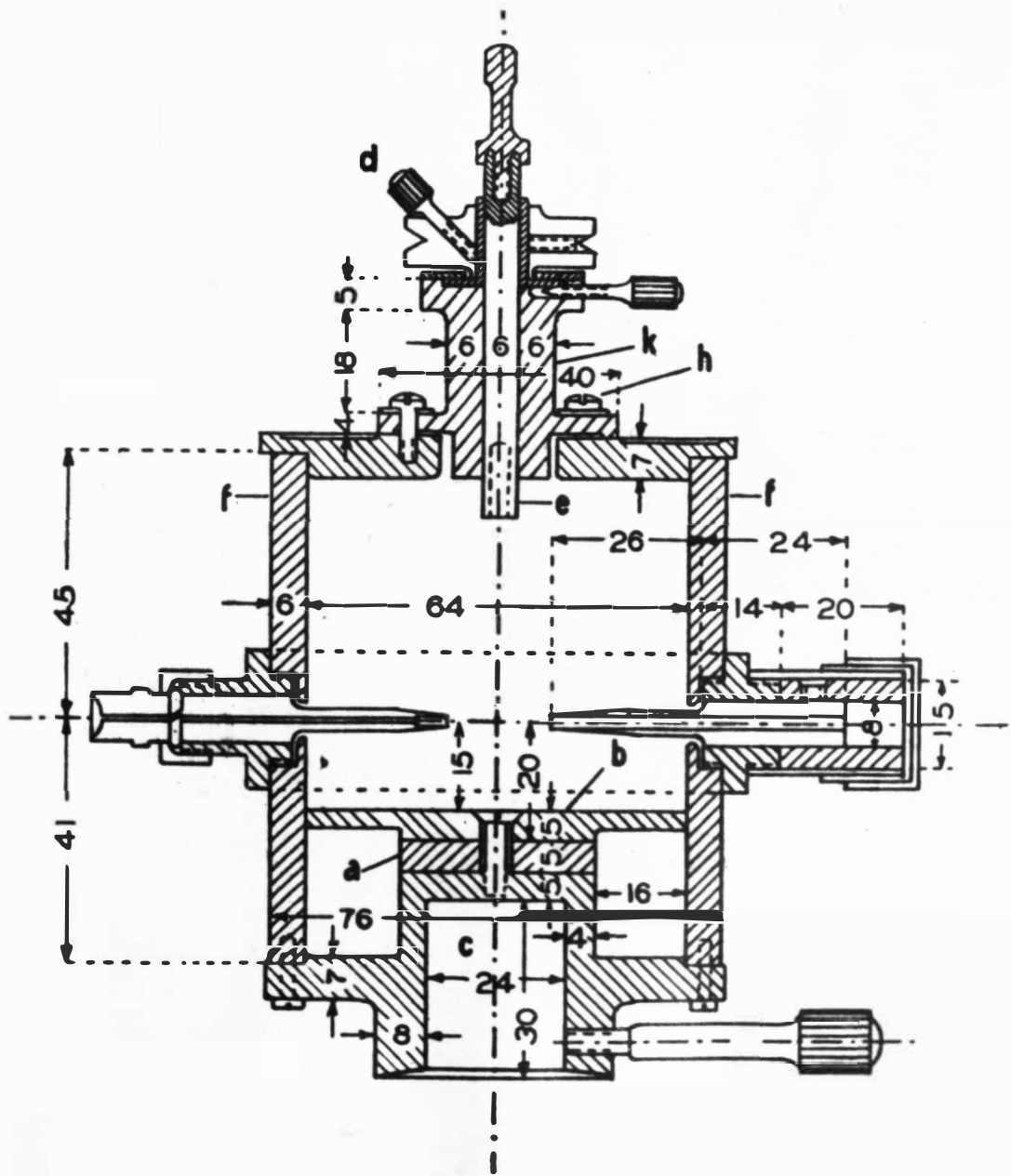


Figure 8. The precision camera.
(Dimensions are given in mm.)

2. X-ray Machine and Temperature Control System

X-ray Machine. A crystalline substance can diffract X-rays and produce a sufficient number of diffraction lines, if the wave length of the X-ray beam used is smaller than the lattice spacings of the crystalline substances. By changing the target of the tube, X-ray beams of different wave lengths can be obtained. The targets are made of different metals, such as chromium, molybdenum, iron, copper, nickel, and cobalt, and are cooled with water during the operation of the X-ray tube. The X-ray machine used in this laboratory was manufactured by the Picker X-ray Corp., and was designed for the production of soft radiation X-rays. The machine is equipped with a clock-switch which shuts off the machine if the flow of cooling water to the target is by some means discontinued. This device protects the target of the X-ray tube from damage, as well as the whole machine.

Temperature Control System In the determination of lattice constants with highest precision, an exact knowledge of the temperature of the sample is important. It should be closely controlled, because small temperature fluctuations affect the magnitude of the lattice spacings. A small change of temperature, even 0.1° C, can influence the lattice constant in the fifth decimal place. Therefore, precision determination must be conducted with thermostats, as the room temperature may vary by some degrees during the occasional long exposures. One more application of the

thermostat is to change the temperature at certain intervals in order to determine the variation of lattice constants with temperature and to compute the thermal expansion coefficient of the substance. In the present investigation, the temperature of the specimens was controlled by a temperature control system which consists of three integral parts, namely, the thermostatic jacket in which the camera was placed, the thermostatic bath, and the cooling water bath.

The thermostatic jacket is a metallic container with a door, and having water channels of 12 mm. in diameter bored lengthwise through the container's walls. The first step was to lock the camera in the jig, thus obtaining a good heat exchange (Fig. 9). Then the whole was placed in the jacket (Fig. 10), and secured to the bottom of the jacket by means of a set screw. The temperature of the jacket (with the camera inside) was maintained by a water stream of constant temperature, circulating from the thermostatic bath up through the channels in the walls of the jacket. The cooling water bath was only used when working below room temperatures. Two diametrically opposite holes, as inlets and outlets for X-rays were provided in the jacket. Two more holes were drilled on the right hand side of the jacket; one of these holes being used to insert the shaft for the rotation of the sample inside of the camera (connected by means of a fork with the cam of the camera shown in Fig. 9, (3)) and the other hole for inserting a thermometer into the thermostatic jacket. A thermometer

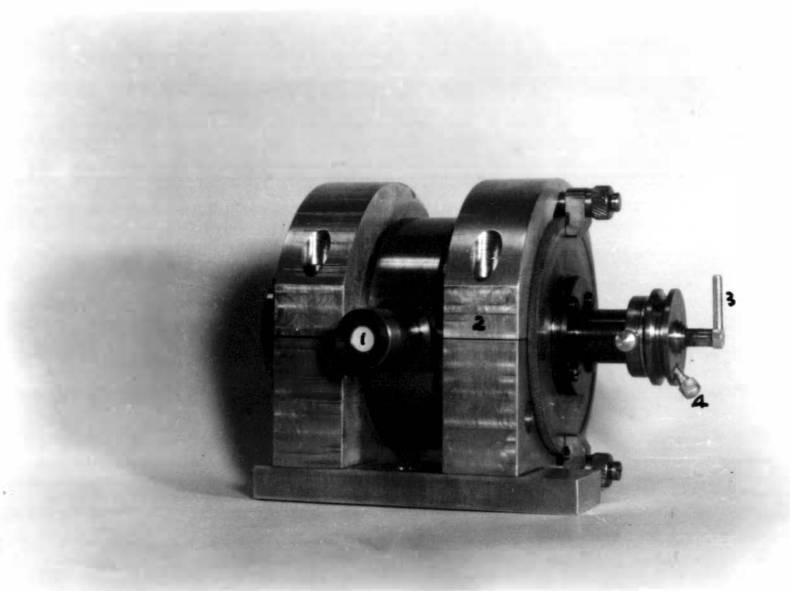


Figure 9. The camera locked in a metallic jig for fixing in the thermostatic jacket.

(1). Fluorescent camera screen on the exit port of X-rays; (2). The jig; (3). The cam of the specimen-rotation shaft; (4). The set screw for adjustment of the position of the specimen.

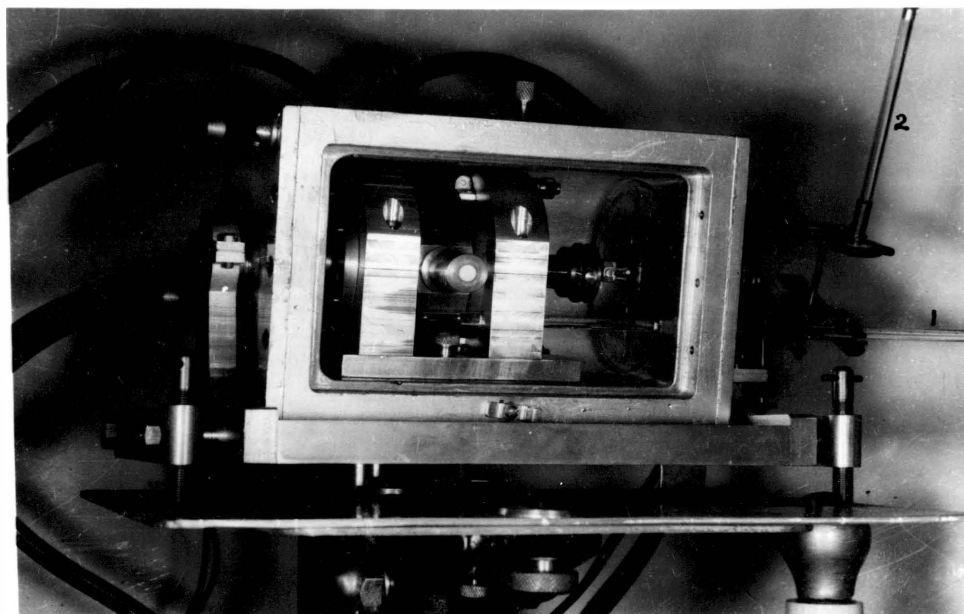


Figure 10. The camera placed in the thermostatic jacket with door removed.

(1). Calibrated thermometer; (2). Magnifying lens for reading the thermometer scale.

with an accuracy of 0.02° C was used in order to measure the accurate temperature of the camera and sample inside the jacket. After the door of the jacket was closed (Fig. 11), the equipment was left until the inside of the jacket (with the loaded camera) had reached the required temperature. Then it was left for an additional hour to be sure that the sample inside the camera had assumed the same temperature as shown by the thermometer.

The constant temperature in the jacket was maintained by a circulating thermostatic bath which was a five gallon porcelain water container. The temperature of the water

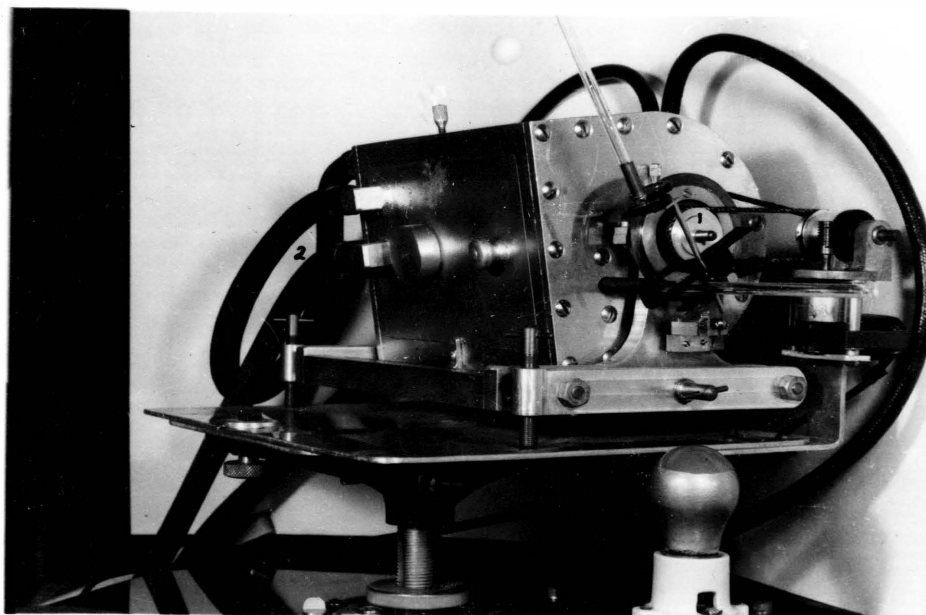


Figure 11. A view of the thermostatic jacket with the door closed.

- (1). Pulley for rotation of specimen;
- (2). Rubber hoses for circulating water of a constant temperature into the jacket.

circulating through the jacket was controlled by an immersion-type, adjustable contact thermoregulator connected with a Fisher-Serfass electronic relay. This bath was connected with the channels of the jacket by one-half inch inside diameter rubber hoses. During the work, the water of the bath was continuously pushed through the channels of the jacket by means of a centrifugal pump, whose speed could be regulated with a variable transformer. As the circulation of the water agitated the bath, no stirrer was necessary. The bath was heated by an adjustable 500 watt heater. For working above room temperature, the heater was plugged into the proper socket of the relay, and the thermo-regulator then maintained the desired temperature in the thermostatic jacket. Under these conditions, the air of the room acted as a cooling medium. The thermo-regulator just mentioned had a sensitivity of 0.02° F, over a range of 50° to 200° F. Figure 12 shows the centrifugal pump (a), the thermoregulator (b), and the heater (c), on the cover of the thermostatic bath (B), and controlling devices on the switchboard (E).

The exposures were required to be made below room temperature, a cooling water bath (Fig. 12 C) was used. The bath consists of a porcelain water container connected with an adjustable refrigerator (Fig. 12 D) and was used to keep the temperature of the bath B below that of the room. The temperature of the said bath was regulated by

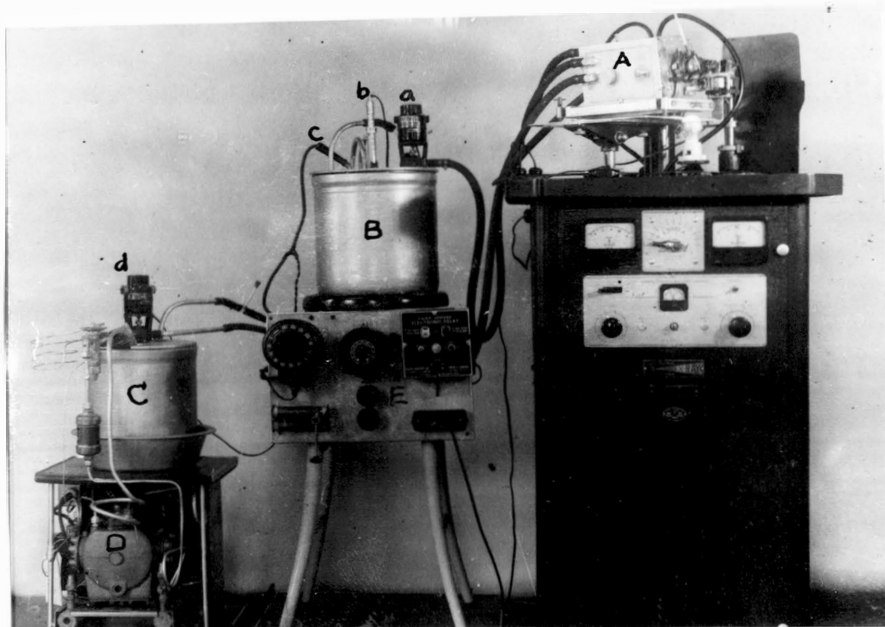


Figure 12. The arrangement of the complete X-ray diffraction unit.

- (A). Thermostatic jacket with the camera inside;
- (B). Thermostatic bath; (C). Cooling water bath;
- (D). Refrigerator; (E). Switchboard;
- (a) and (d). Centrifugal pumps;
- (b). Thermo-regulator; (c). Heater.

a one-half inch copper coil, through which cooling water was driven by a second pump (Fig. 12 d). The speed of this pump could also be regulated by a variable rheostat. For working below room temperatures, the pump was plugged into the other socket of the electronic relay and now air of the room acted as the heating medium. The thermo-regulator worked as well as it did for temperatures above room temperatures.

3. Comparator

The purpose of measuring positions of diffraction lines on the X-ray films is to calculate Bragg angles, and then the lattice constant of the sample. The comparator is the mechanical device used for measuring the X-ray films and is supplied with an exact micrometer screw.

The comparator (Fig. 13) used in this laboratory was manufactured by D. Mann of Lincoln, Massachusetts. It has a travelling carriage, and a microscope in a fixed frame mounted above the carriage. The microscope, of a low magnification, has an objective lens with cross hairs. The screw has a pitch of 1 mm., and the micrometer drum, connected to the screw has 1000 divisions. By this device, the positions of the diffraction lines, if they are sharp enough, can be measured with an accuracy of 0.001 mm. The film has to be adjusted correctly on the carriage by means of two screws. An adjustment is correct when the center of the cross hairs were exactly on the central line of the film.

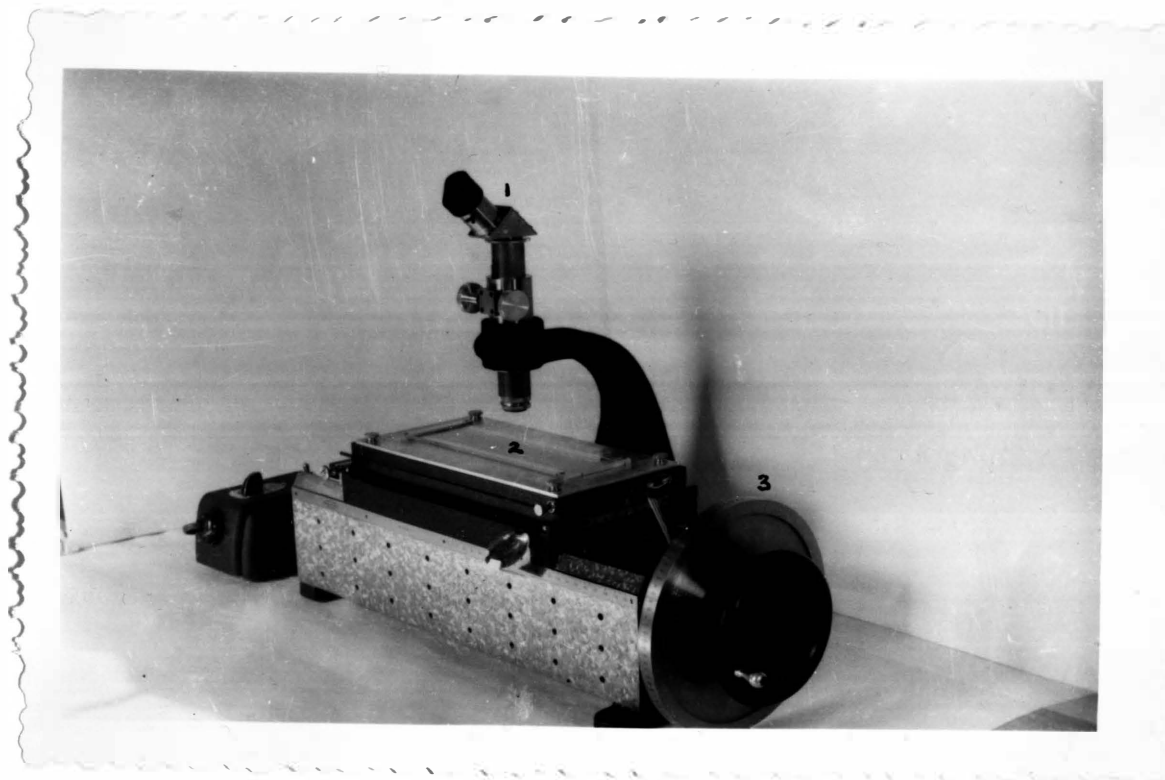


Figure 13. The Comparator.

- (1). Microscope; (2). Film for measuring;
(3). Micrometer drum.

INDEXING AND MEASURING THE FILM

1. Theory

As mentioned above, the purpose of making and measuring the X-ray films is to find the Bragg angle θ of the diffraction lines and to calculate the exact lattice constant of the substance. The diffraction phenomena can be explained by the familiar Bragg equation:

$$N \lambda = 2 d \sin \theta \quad (1)$$

In this equation, N (the order of diffraction), λ (the wave length of the X-ray), and θ (Bragg angle of the diffraction spots) are used to find the value for d , which is the interplanar spacing of the substance under investigation; d has a close relationship to a (lattice constant), according to the equation:

$$d = \frac{a}{\sqrt{h^2 + k^2 + l^2}} \quad (2)$$

By substituting equations (2) for d in (3), Bragg formula for the calculation of lattice constants is obtained:

$$a = \frac{\lambda \sqrt{h^2 + k^2 + l^2}}{2 \sin \theta} \quad (3)$$

In (3), the order of refraction is already multiplied by corresponding crystallographic indices. This equation clearly shows that for the precise determination of lattice constants, the accuracy of a depends only upon the angle θ , as the correct Miller index is an integer, and

can be correctly obtained, while the wave length used is already known and determined with greatest precision.

Bragg angle θ (or \mathcal{D}) used in equation (3) can be either under small angles in the front reflection or under large angles ϕ (or φ) in the back reflection (Fig. 14).

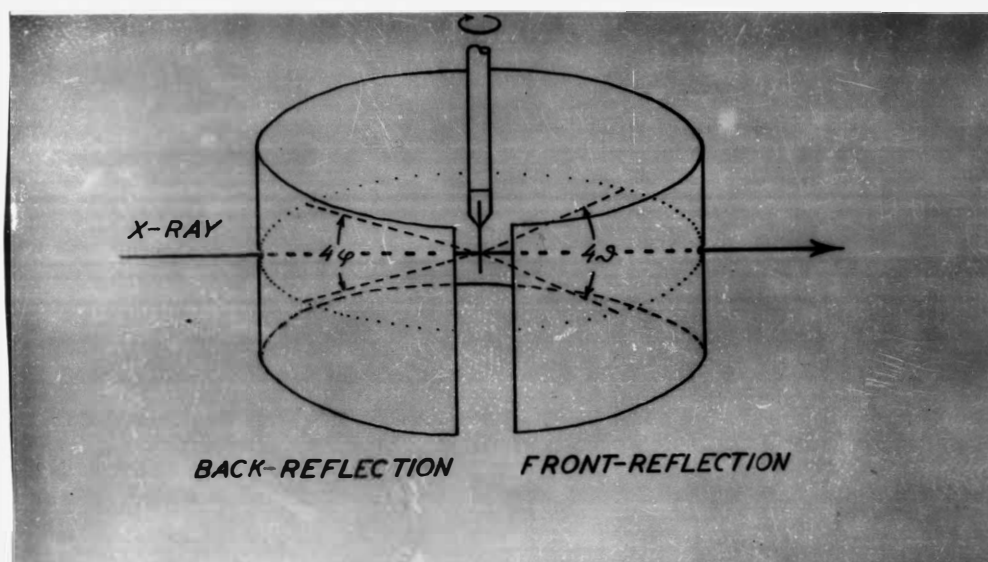


Figure 14. The film arrangement in the asymmetric method.

\mathcal{D} , the Bragg reflection angle;
 φ , the back reflection angle.

When θ is very large, i.e., nearly 90° , a small error in measuring gives only a small deviation in the value for $\sin \theta$, and will not affect the precision of the lattice determination too much. So interferences under large Bragg angles in the back reflection region are necessary for the determination of precise lattice constants. One more advantage in using large glancing angle θ is to reduce the

error due to absorption nearly to zero, and therefore, the shift of diffraction lines can be entirely neglected.

Figure 14 shows that ϕ , the back reflection angle, is complementary to θ , which is the front reflection angle. The Bragg formula for the calculation of lattice constants from back reflection lines then becomes:

$$a = \frac{\lambda \sqrt{h^2 + k^2 + l^2}}{2 \cos \phi} \dots \dots (4)$$

$$\text{where } \phi = 90^\circ - \theta$$

2. Indexing the Film and Selection of the Target

The purpose of indexing the film is to find the Miller indices of the diffraction lines, in order to determine the lattice constants of the specimen. Besides this, it also helps to find the structure type and the atomic position of the sample. A convenient, graphical method, based on the principle of reciprocal lattice, ⁽⁹⁾ was used for indexing the cubic pattern in this research. In Figure 15 the cross section of the Debye-Scherrer camera is shown, indicating the path of the direct and reflected X-ray beams. From the figure, it follows directly:

$$\frac{X}{2r} = \sin \theta \dots \dots (5)$$

$$\text{and } \frac{P}{X} = \sin \theta \dots \dots (6)$$

Considering the inside wall of the camera as the sphere of reflection, the chord X represents the reciprocal lattice

(9) Straumanis, M., Zeit Krist, p. 104, 167, 1942

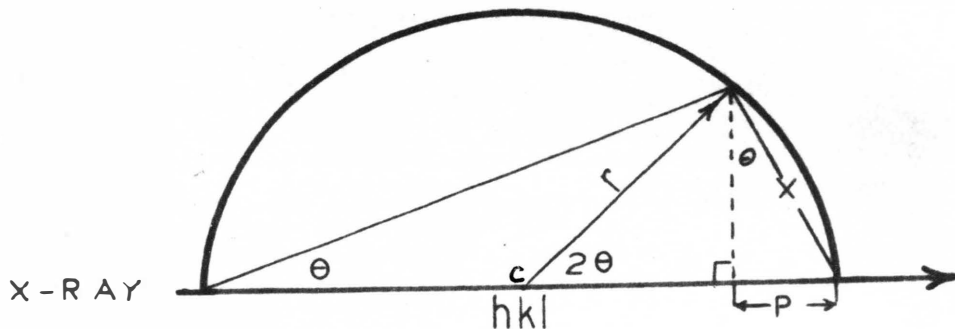


Figure 15. Path of the X-ray beam in a Debye-Scherrer camera.

- c, the powder sample;
- X, vector of the reciprocal lattice;
- P, projection of the reciprocal lattice vector X on the diameter of the camera;
- r, radius of the camera.

vector of the three dimensional reciprocal lattice. Thus, P is the projection of X on the diameter of the camera.

From the Bragg equation,

$$\lambda = 2d \sin \theta, \text{ if } N = 1$$

It follows that:

$$a^2 = \frac{\lambda^2 \sum h^2}{4 \sin^2 \theta} \dots \dots \dots (7)$$

$$\text{where } \sum h^2 = (h^2 + k^2 + l^2)$$

By various combinings of the equations (5) (6) and (7), one can obtain,

$$P = \frac{r \lambda^2}{2 a^2} \sum h^2 \dots \dots \dots (8)$$

As $\frac{r \lambda^2}{2 a}$ is constant for the particular cubic sample and radiations, it follows from equation (8):

$$P = k \sum h^2 \quad (9)$$

Since the length of P, as obtained from other lines on the reflection circle, is proportional to $\sum h^2$, representing the integers 1, 2, 3, 4, etc., all differences of the projection P of the subsequent reciprocal lattice vectors of a cubic substance are equal. There are no corresponding lines for $\sum h^2$, which cannot be split into integers of squares.

A reflection circle on a bigger scale, corresponding to the inside wall of a Debye-Scherrer camera, is shown in Figure 16. As an arbitrary camera, radius for copper radiation 100 mm. (10) was chosen, and the radii for other radiations are obtained as follows:

If the smallest P is equal to P_{\min} , resulting in $\sum h^2 = 1$, then

$$a = \lambda \sqrt{\frac{r}{P_{\min}}} \quad (10)$$

Now, if P is kept constant, the change in radiation from λ_1 to λ_2 will result in a changed radius (r_2) of the reflection circle:

$$r_2 = r_1 \frac{\lambda_1^2}{\lambda_2^2} \quad (11)$$

(10) Straumanis, M., Am. Mineralogist, p. 37, 48, 1952

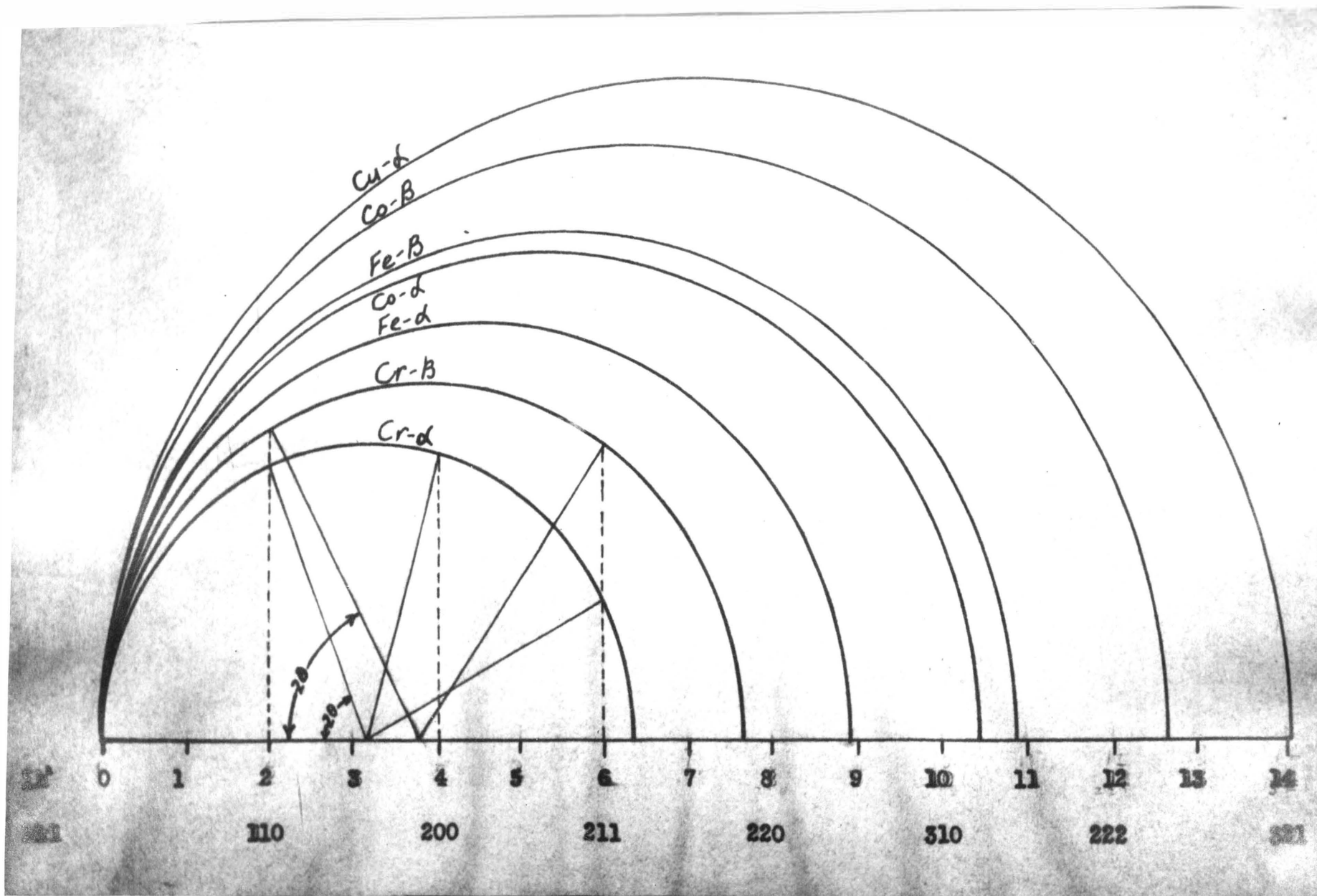


Figure 16. The graphic method for indexing film and selecting radiation
(Powder chromium)

where r_2 , the radius of new radiation reflection circle.

r_1 , the radius of Cu-K α_1 radiation reflection circle.

λ_2 , the wave length of new radiation.

λ_1 , the wave length of Cu-K α_1 radiation.

If the radius of Cu-K α_1 radiation is taken as 100 mm., then for other radiations are obtained as follows:

$$\text{For Cu-K}\beta_1, \quad r_2 = 100 \times \frac{\lambda_1^2}{\lambda_2^2} = 100 \times \frac{(1.5374)^2}{(1.3894)^2} = 121.3 \text{ mm.}$$

$$\text{For Cr-K}\alpha_1, \quad r_2 = 100 \times \frac{\lambda_1^2}{\lambda_2^2} = 100 \times \frac{(1.5374)^2}{(2.2850)^2} = 45.3 \text{ mm.}$$

$$\text{For Cr-K}\beta_1, \quad r_2 = 100 \times \frac{\lambda_1^2}{\lambda_2^2} = 100 \times \frac{(1.5374)^2}{(2.0806)^2} = 54.6 \text{ mm.}$$

In Figure 16, the reflection circles for different radiations are drawn. A trial photograph was made with Cr-radiation and so this reflection circle was taken as the base circle. The angles 2θ , as measured from the film, are tabulated in Table III. They start from the origin O and are projected to a diameter of 200 mm. The distances from the origin O to the projection points are divided into the largest possible division (equal P_{\min}), so that the end point of any one projection from the origin O is an integral multiple of P_{\min} . This can be done by trial. The numerical number of a projection point is the Σh^2 of the

Table III
Values of the diffraction lines
Cr- radiation

<u>No. of line</u>	<u>2 θ (degree)</u>	<u>K-radiation</u>	<u>h k l</u>
2	61.627	β	1 1 0
2	68.458	α	1 1 0
4	105.241	α	2 0 0
6	124.661	β	2 1 1
6	152.885	α_1	2 1 1
6	153.736	α_2	2 1 1

Miller indices of the corresponding reflection lines.

Indexing of the film can also be made mathematically as shown in Table IV, but it is not so convenient as the graphical method just mentioned. In selecting a proper radiation, the radiation whose reflection circle intersects closest to a P division is the best. In Figure 16, the best radiation for chromium is copper and next, chromium. The glancing angle due to the copper radiation, however, is too large, i.e., nearly 90° , and is inside the collimator, and so cannot be seen on the film. Therefore, chromium was selected as the proper radiation in the measurements.

TABLE IV

MATHEMATICAL INDEXING METHOD OF PURE CHROMIUM, CR-RADIATION

No. of Line	R-L	$\theta =$ F(R-L)*	Sin θ	$d = \frac{\lambda}{2 \sin \theta}$			$\sqrt{2h^2} = \frac{a}{d}$			Calculated $h^2+k^2+l^2$			hkl
				α_1	α_2	β_1	α_1	α_2	β_1	α_1	α_2	β_1	
1	68.464	30.814	0.51225	2.2304	2.2343	2.0308	1.2904	1.2881	1.4172	1.6651	1.6592	<u>2.0085</u>	110 β_1
2	76.052	34.229	0.56250	2.0311	2.0347	1.8494	1.4180	1.4145	1.5562	2.0107	<u>2.0008</u>	2.4218	110 α_1
3	83.054	52.621	0.79463	1.4378	1.4403	1.3091	2.0017	1.9982	2.1985	<u>4.0068</u>	3.9928	4.8334	200 α_1
4	61.428	62.331	0.88564	1.2900	1.2923	1.1746	2.2310	2.2270	2.4502	4.9774	4.9595	<u>6.0035</u>	211 β_1
5	30.158	76.428	0.97208	1.1753	1.1774	1.0702	2.4487	2.4444	2.6898	<u>5.9961</u>	5.9751	7.2318	211 α_1
6	29.179	76.868	0.97385	1.1732	1.1752	1.0682	2.4531	2.4489	2.6943	6.0177	<u>5.9971</u>	7.2593	211 α_2

* 0.45007, calculated by the same method as in Table V.

3. Measurement of the Film

Diffraction lines on the film are measured by a comparator, as mentioned before. Each pair of lines was carefully measured three times in order to eliminate the visual error, and the average value used to calculate the Bragg angle θ . How to calculate can be explained by a simple sketch as shown in Figure 17.

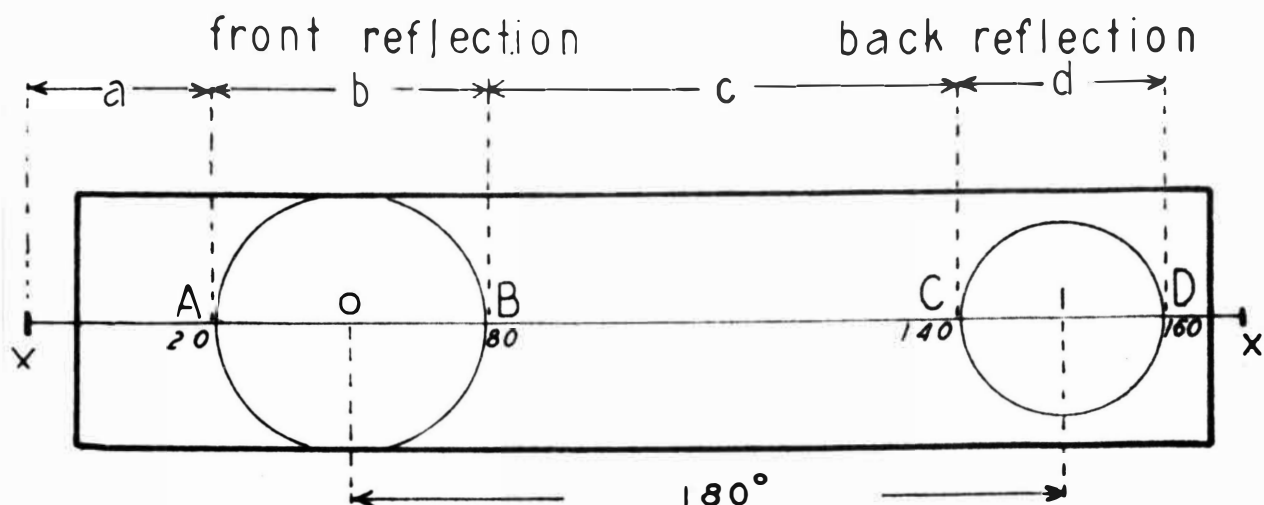


Figure 17. Schematic diagram of a simplified asymmetric powder pattern.

Suppose A, B, and C, D, are the corresponding pairs of lines, appearing in front-reflection and back-reflection regions. These rings are not circular, yet they are symmetrical to the outlet and inlet holes I and O on the film, although the symmetry lines of each pair of reflection may, or may not, coincide with the exact centers of the holes. The line X-X¹ in Figure 16 represents a millimeter scale, on which the film may be laid flat. Such a

film is measured as follows: The effective film circumference is equal to $(\overline{XD} + \overline{XC}) - (\overline{XB} + \overline{XA}) = 201 = 360^\circ$; assuming that $(\overline{XD} + \overline{XC}) - (\overline{XB} + \overline{XA}) = 200$ mm., and 1 mm. on the film will be equal to 1.8 degree. As the angle measured is four times the glancing angle, so the factor $F = \frac{1.8}{4} = 0.45$ will be obtained for conversion of the measured angular distances on the film into degree, in term of glancing angles. For example, if the distance between the lines of an interference pair is 10 mm., then the glancing angle is $10 \times 0.45 = 4.5$ degrees. If the angle is in the front reflection region, then it is θ and is equal to 4.5 degrees. If the interference lines are in the back reflection region, then the angle measured is $\phi = 4.5^\circ$ degrees. The front reflection angle for the same pair then will be: $\theta = 90 - 4.5 = 85.5$ degrees, because such a line lies in the back reflection region. The back reflection angle, for the interference $211 \alpha_1$, was used for the determination of lattice constants of chromium. An X-ray powder photograph of this metal is shown in Figure 18, and its measurement and calculation is given in Table V.

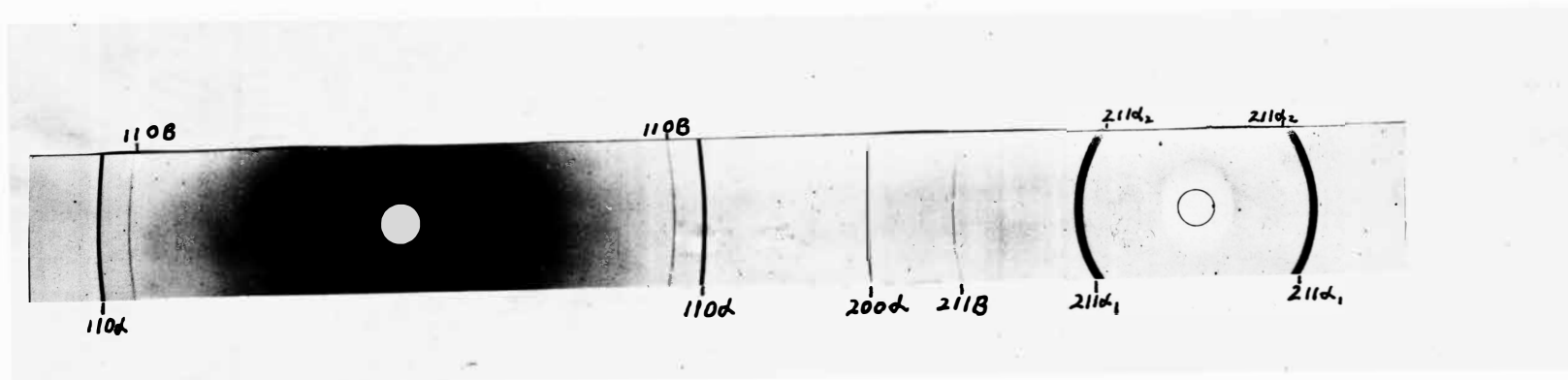


Figure 18. X-ray powder photograph of chromium sample with chromium radiation.

TABLE V

Record of Film Measurement and Calculation of Pure Chromium
Chromium Radiation Room Temperature

Intensity h k l	<u>Front Reflection</u>		<u>Back Reflection</u>				
	w. (β)	s. (α)	m. (α)	v.w. (β)	v.s. (α_1)	s. (α_2)	
	110	110	200	211	211	211	
Comp. Read.	(B) 86.985	90.790	(D) 194.271	183.560	167.825	167.332	
Comp. Read.	(A) 18.521	14.737	(C) 111.217	122.080	137.667	138.153	
	<u>B+A</u> 105.506	<u>105.527</u>	<u>D+C</u> 305.488	(305.640)	<u>305.492</u>	<u>305.485</u>	
	105.516(Ave. B+A)		305.488(Ave. D+C)				
$305.488 - 105.516 = 199.972 \text{ mm.} \approx 360^\circ$ $1 \text{ mm.} = 1.80028^\circ (4\phi)$ $\text{or, } 1 \text{ mm.} = 0.45007^\circ (\phi) = F$							
B - A mm.	68.464	76.053	D-C mm.	83.054	61.480	30.158	29.179
(B - A) F	30.814	34.229	ϕ°	37.380	27.670	13.573	13.133
Sin θ or Cos θ	0.51225	0.56250		0.79463	0.88564	0.97208	0.97385
$\frac{\lambda}{2} \sqrt{\sum h^2}$				not used		2.79859	2.80334
a, in kX						2.87897	2.87861

EXPERIMENTAL RESULTS

1. Lattice Constant

X-ray photographs to determine the exact value of the lattice constant of chromium were made with chromium powder, at ten degree intervals between 10° and 50° C. For each sample, three photographs were taken at every temperature, and the average value of the three lattice constants was considered to be the correct constant at that temperature. The lattice constants of four chromium samples are listed in Tables VI to X and the changes of the lattice constants with the temperatures are shown in Figs. 19 to 22.

TABLE VI

Lattice Constants of Electrolytic Chromium
at Different Temperatures

Film No.	Temp (°C)	$\rho_{211}\alpha_1$ in degrees	Lattice Constants in kX	Lattice Constant A_t in kX (Average)
788	13.0	13.548	2.87870	
789	13.0	13.570	2.87897	2.87886
790	13.0	13.567	2.87891	
791	20.0	13.578	2.87905	
792	20.0	13.580	2.87908	2.87905
793	20.0	13.576	2.87903	
794	30.0	13.584	2.87911	
795	30.0	13.593	2.87923	2.87918
796	30.0	13.590	2.87920	
797	40.0	13.591	2.87920	
798	40.0	13.607	2.87941	2.87928
799	40.0	13.592	2.87923	
800	50.0	13.593	2.87923	
801	50.0	13.625	2.87962	2.87947
802	50.0	13.620	2.87958	

TABLE VII

Lattice Constants of Sintered Electrolytic Chromium
at Different Temperatures

Film No.	Temp. (°C)	$\theta_{211\alpha_1}$ in degrees	Lattice Constants in kX	Lattice Constant A_1 in kX (Average)
811	10.0	13.563	2.87888	
810	10.0	13.554	2.87876	2.87885
809	10.0	13.566	2.87891	
808	30.0	13.581	2.87908	
807	30.0	13.568	2.87894	2.87905
806	30.0	13.586	2.87914	
805	50.0	13.619	2.87956	
804	50.0	13.615	2.87950	2.87951
803	50.0	13.613	2.87947	

TABLE VIII

Lattice Constants of Iodide-Cr Low in Metallic
Impurities at Different Temperatures

Film No.	Temp. (°C)	$\varphi_{211\alpha_1}$ in degrees	Lattice Constants in kX	Lattice Constant A ₁ in kX (Average)
756	11.6	13.569	2.87894	
757	11.7	13.555	2.87876	2.87885
758	11.7	13.561	2.87885	
753	13.0	13.569	2.87894	
754	13.0	13.543	2.87864	2.87874
755	13.0	13.554	2.87876	
759	20.0	13.587	2.87917	
760	20.0	13.554	2.87876	2.87898
761	20.0	13.576	2.87903	
765	30.0	13.591	2.87920	
766	30.0	13.582	2.87911	2.87913
767	30.0	13.580	2.87908	
762	40.0	13.599	2.87929	
763	40.0	13.573	2.87901	2.87916
764	40.0	13.587	2.87917	
768	50.0	13.605	2.87938	
769	50.0	13.609	2.87944	2.87937
770	50.0	13.597	2.87929	

TABLE IX

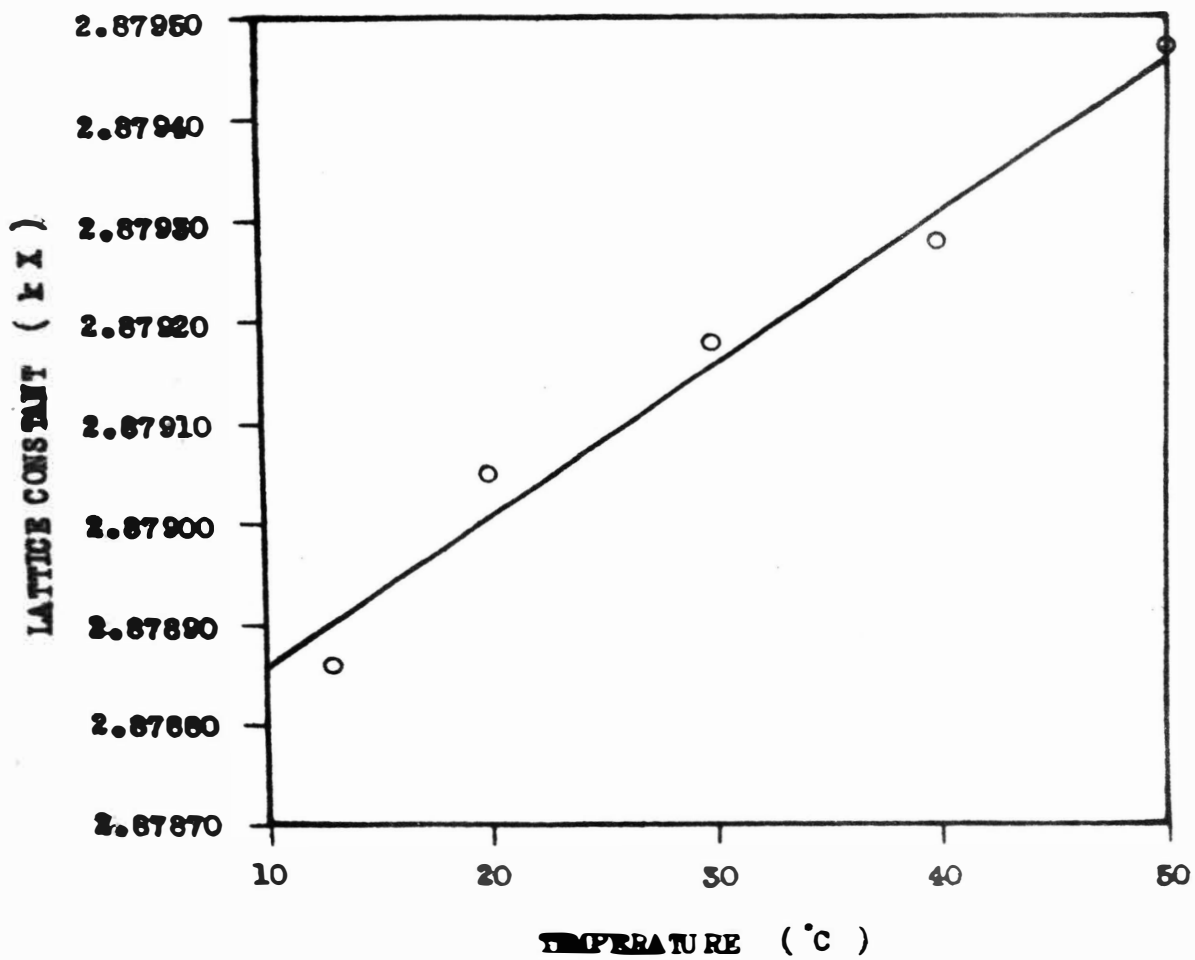
Lattice Constants of Iodide-Cr Low in Non-Metallic
Impurities at Different Temperatures

Film No.	Temp. (°C)	$\psi_{211\alpha_1}$ in degrees	Lattice Constants in kX	Lattice Constant A_{\dagger} in kX (Average)
787	13.0	13.551	2.87873	
786	13.0	13.553	2.87876	2.87876
785	13.0	13.556	2.87879	
783	20.0	13.576	2.87903	
782	20.0	13.579	2.87905	2.87902
781	20.0	13.570	2.87897	
780	30.0	13.577	2.87903	
779	30.0	13.588	2.87917	2.87909
778	30.0	13.581	2.87908	
777	40.0	13.594	2.87923	
776	40.0	13.591	2.87920	2.87921
775	40.0	13.590	2.87920	
774	50.0	13.605	2.87938	
773	50.0	13.613	2.87947	2.87945
772	50.0	13.616	2.87950	

TABLE X

Lattice Constants of Four Chromium Samples
at Different Temperatures

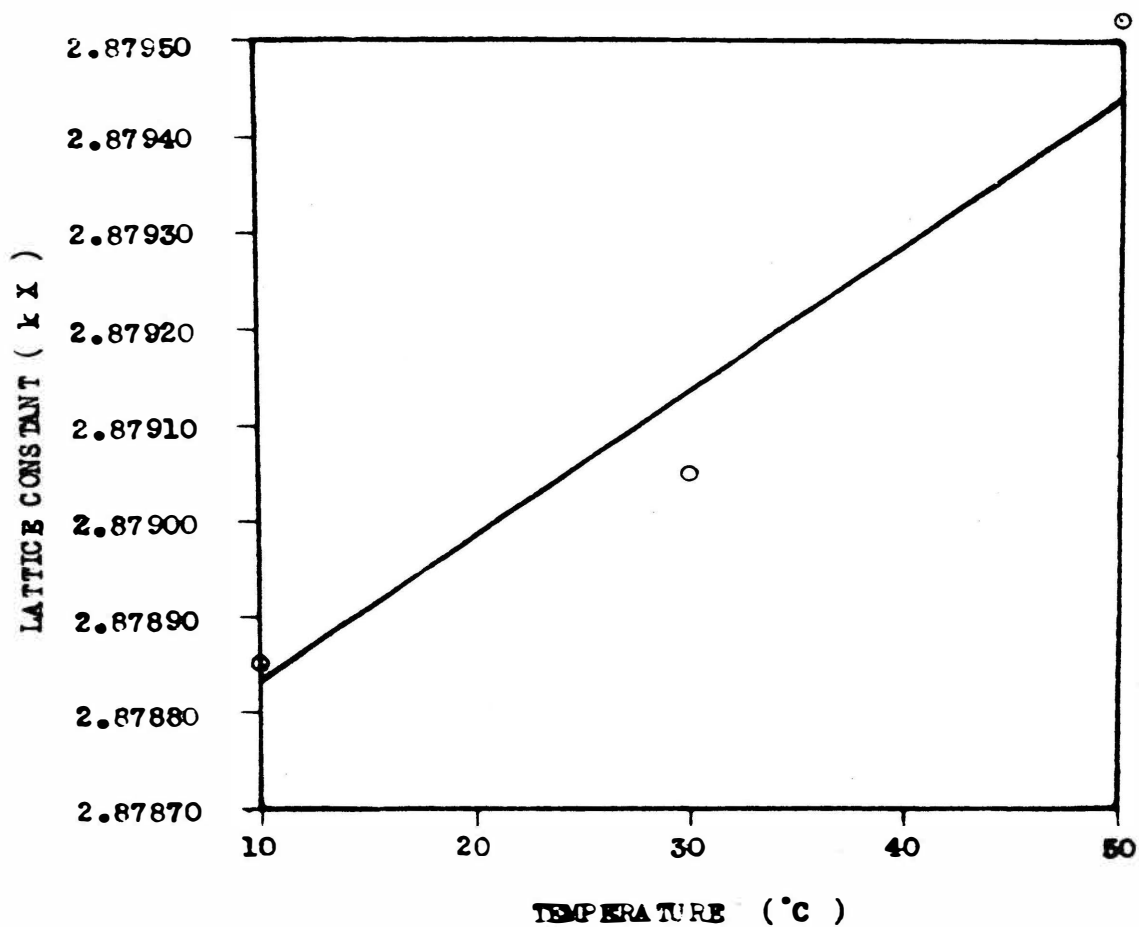
Sample	10° C	20° C	30° C	40° C	50° C
Electrolytic	2.87886(13°)	2.87905	2.87918	2.87928	2.87947
Sintered Electrolytic	2.87885(10°)	- -	2.87905	- -	2.87951
Iodide (Low Metallic)	2.87898(12°)	2.87898	2.87913	2.87916	2.87937
Iodide (Low Non- Metallic)	2.87876(13°)	2.87902	2.87909	2.87921	2.87945
Average	2.87886(12°)	2.87902	2.87911	2.87922	2.87945



LATTICE CONSTANTS OF ELECTROLYTIC-CR

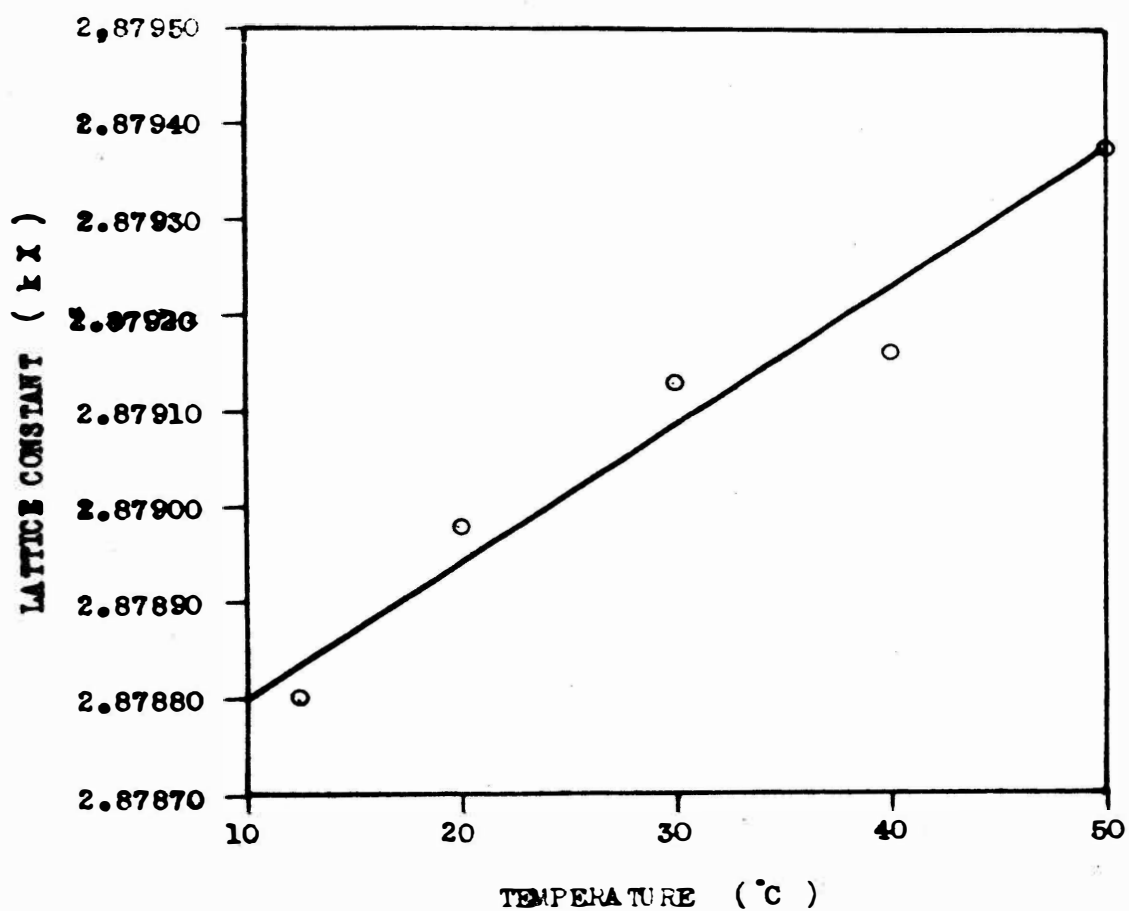
AT DIFFERENT TEMPERATURES

FIGURE 19



LATTICE CONSTANTS OF SINTERED ELECTROLYTIC-CR
AT DIFFERENT TEMPERATURES

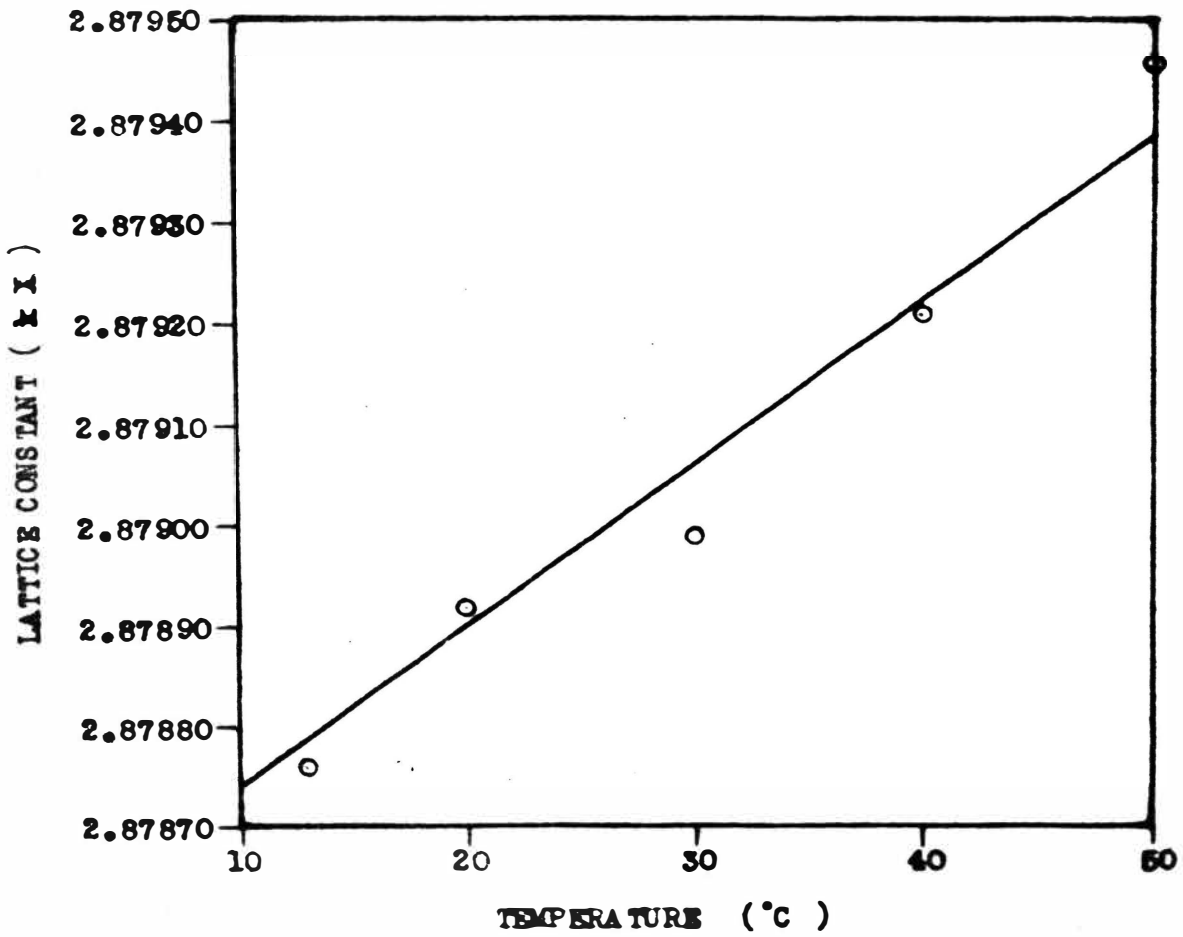
FIGURE 20



LATTICE CONSTANTS OF IODIDE-CR (LOW METALLICS)

AT DIFFERENT TEMPERATURES

FIGURE 21



LATTICE CONSTANTS OF IODIDE-CR (LOW NON METALLICS)

AT DIFFERENT TEMPERATURES

FIGURE 22

2. Coefficient of Expansion

The coefficient of thermal expansion of chromium was calculated from the average lattice constants at different temperatures, using the following equation:

$$\alpha = \frac{a_{t_2} - a_{t_1}}{a_{t_1}(t_2 - t_1)} \dots \dots \dots (12)$$

α , being the linear coefficient of thermal expansion

a_{t_2} being lattice constant at temperature t_2

a_{t_1} being lattice constant at temperature t_1

The accurate coefficient of thermal lattice expansion is obtained by taking the average value⁽¹¹⁾ of all possible combinations of lattice constants at 10°, 20°, 30°, 40°, and 50° C. This value is considered to be the most probable coefficient of thermal expansion of the respective samples between 10° and 50° C. The method of calculation is shown in the sample of sintered electrolytic chromium:

$$a_{50} = 2.87951, \quad a_{30} = 2.87905, \quad a_{10} = 2.87885$$

$$\alpha_{(50-30)} = \frac{a_{50} - a_{30}}{a_{30}(50-30)} = \frac{2.87951 - 2.87905}{2.87905 \times 20} = 7.99 \times 10^{-6}$$

$$\alpha_{(50-10)} = \frac{a_{50} - a_{10}}{a_{10}(50-10)} = \frac{2.87951 - 2.87885}{2.87885 \times 40} = 5.73 \times 10^{-6}$$

$$\alpha_{(30-10)} = \frac{a_{30} - a_{10}}{a_{10}(30-10)} = \frac{2.87905 - 2.87885}{2.87885 \times 20} = 3.47 \times 10^{-6}$$

(11). Straumanis, M., anorg Chem., p. 238, 175, 1938.

$$\text{Average } \alpha_{(10-50)} = \frac{1}{3} (7.99 + 5.73 + 3.47) = 5.73 \times 10^{-6}$$

The average coefficients of thermal expansion obtained for four different chromium samples, ranged from 4.92×10^{-6} to 6.14×10^{-6} , between the temperature range of 10° and 50° C, as shown in Tables XI to XV. These figures are very close to the results obtained by Hidnert,⁽⁸⁾ ranging from 5.2×10^{-6} to 6.6×10^{-6} in the temperature range of 20° and 60° C. Neither inflection points near 38° C, as obtained by MacNair,⁽²⁾ nor a minimum in the coefficients of expansion near 37° C, as found by Fine,⁽¹⁾ were observed.

TABLE XI

Coefficient of Thermal Expansion of Electrolytic Chromium
Between 13° and 50° C. See Table VI.

Combinations	Δt	$\alpha \cdot 10^{-6}$
50 - 40	10	6.60
50 - 30	20	5.04
50 - 20	30	4.86
50 - 13	37	5.73
40 - 30	10	3.47
40 - 20	20	3.99
40 - 13	27	5.40
30 - 20	10	4.51
30 - 13	17	6.54
20 - 13	7	9.43
Average	-	5.56

TABLE XII

Coefficient of Thermal Expansion of Sintered Electrolytic Chromium Between 10° - 50° C. See Table VII.

Combinations	Δt	$\alpha \cdot 10^{-6}$
50 - 30	20	7.99
50 - 10	40	5.73
30 - 10	20	3.47
Average	-	5.73

TABLE XIII

Coefficient of Thermal Expansion of Iodide-Chromium (Low Metallic) Between 12° and 50° C. See Table VIII.

Combinations	Δt	$\alpha \cdot 10^{-6}$
50 - 40	10	7.29
50 - 30	20	4.17
50 - 20	30	4.51
50 - 12	38	5.21
40 - 30	10	1.04
40 - 20	20	3.13
40 - 12	28	4.47
30 - 20	10	5.21
30 - 12	18	6.37
20 - 12	8	7.81
Average	-	4.92

TABLE XIV

Coefficient of Thermal Expansion of Iodide-Chromium
(Low Non-Metallic) Between 13° and 50° C.

See Table IX.

Combinations	Δt	$\alpha \cdot 10^{-5}$
50 - 40	10	8.34
50 - 30	20	6.25
50 - 20	30	4.98
50 - 13	37	6.48
40 - 30	10	4.17
40 - 20	20	3.30
40 - 13	27	5.79
30 - 20	10	2.43
30 - 13	17	6.74
20 - 13	7	12.90
Average	-	6.14

TABLE XV

Coefficient of Thermal Expansion of Four Different
Kinds of Chromium Samples Between 10° and 50° C.

Chromium Sample	Ave. coeff. of expansion $\alpha \times 10^{-6}$
Electrolytic	5.56
Sintered electrolytic	5.73
Iodide (low metallics)	4.92
Iodide (low non-metallics)	6.14
Average	5.59

The fluctuations of the lattice constants can now be determined by means of the expansion coefficient (Table XV) after the reduction to 20° of the constants shown in Table X. The equation used was:

$$\alpha = \frac{a_{t_2} - a_{t_1}}{a_{t_1} (t_2 - t_1)} = \frac{a_{20} - a_{t_1}}{a_t \Delta t}$$

$$\text{or } a_{20} = a_t + \alpha a_t \Delta t \quad (13)$$

Sintered electrolytic chromium is taken as an example (See Table VII and Table XII):

	a_t	$\alpha a_t \Delta t$	a_{20} in kX
For 10° C,	$a = 2.87885$	$+ 0.00016$	$= 2.87901$
For 30° C,	$a = 2.87905$	$+ 0.00016$	$= 2.87889$
For 50° C,	$a = 2.87951$	$+ 0.00050$	$= 2.87901$
Average value	$= \frac{1}{3} (2.87901 + 2.87889 + 2.87901)$		
	$= 2.87897 \pm 0.00005$		

Figures for the other three kinds of chromium samples are listed in Table XVI.

3. Correction of Refraction and The Precise Lattice Constants

From a measured glancing angle θ , not the actual lattice constant, but a little smaller value obtained due to the deviation from Bragg's Law. These deviations are greater, the lower the order of the diffraction. The corrected Bragg Equation, as derived by Ewald, ⁽¹²⁾ may be

(12). Wien, W., Handb. d. Experimental Phys., p. 24, 94, 1930.

written as follows:

$$N \lambda = 2 d (1 - 5.40 \rho \frac{d^2}{N^2} 10^{-6}) \sin \theta_N \dots (14)$$

or, for more convenient use:

$$a_0 = a_N (1 + \frac{5.4 a^2 \rho}{N^2 \Sigma h^2} 10^{-6}) \dots (15)$$

where: a_0 , corrected constant
 a_N , experimental constant
 N , order of diffraction
 ρ , density of the crystal
 Σh^2 , quadratic sum of the Miller indexes

Equation (15) is valid only for the symmetrical reflection. The calculation for the refraction correction is as follows:

In this experiment, $a = 2.87942$, $\rho = 7$, $N = 1$, $\Sigma h^2 = 6$

$$\begin{aligned} a_0 &= 2.87942 (1 + \frac{5.4 \times (2.87942)^2 \times 7}{1 \times 6} 10^{-6}) \\ &= 2.87942 (1 + 0.000522) \\ &= 2.87942 + 0.00015 \\ &= 2.87957 \end{aligned}$$

So 0.00015 was taken as the correction for refraction. Figures after correction of refraction for four different kinds of samples are tabulated in Table XVI, and these figures represent the precise lattice constants of chromium at 20° C. Moreover, as Barrett⁽¹³⁾ pointed out that the

(13). Barrett, C. S., Structure of Metals, McGraw-Hill, New York, p. 150, 1952.

refraction should be omitted in lattice constant determination, the correction for refraction in Table XVI is therefore added separately, so that the uncorrected figure is also available.

Table XVI shows that the precise lattice constant of electrolytic chromium at 20° C is $2.87914 \text{ kX} \pm 0.00005$, and of iodide chromium at 20° C, $2.87908 \text{ kX} \pm 0.00007$. These figures are very close to Fine's 2.87900 kX at 20° C and to Wood's 2.8796 kX at 18° C. As iodide chromium is purer than electrolytic chromium (see Table II), the lattice constant of the former is smaller. So the lattice constant of pure chromium becomes larger if impurities are present.

TABLE XVI.

The Precise Lattice Constants of Four Different Chromium Samples

Kind of Sample (Ave. Coeff. of Exp.)	Temp. °C	a_t (kX)	$\alpha a \Delta t$	Reduce to $a_{20^\circ C}$ (kX)
Electrolytic Chromium (5.56×10^{-6})	13	2.87886	+0.00011	2.87897
	20	2.87905	± 0.00000	2.87905
	30	2.87918	-0.00016	2.87902
	40	2.87928	-0.00032	2.87896
	50	2.87947	-0.00048	2.87899
			Average	2.87900 ± 0.00004
		Refraction correction	0.00015	
			<u>2.87915</u>	
Sintered electrolytic Chromium (5.73×10^{-6})	10	2.87885	+0.00016	2.87901
	30	2.87905	-0.00016	2.87889
	50	2.87951	-0.00050	2.87901
			Average	2.87897 ± 0.00005
		Refraction correction	0.00015	
			<u>2.87912</u>	
Iodide Chromium (low metallics) (4.92×10^{-6})	12	2.87880	+0.00011	2.87891
	20	2.87898	± 0.00000	2.87898
	30	2.87913	-0.00014	2.87899
	40	2.87916	-0.00028	2.87888
	50	2.87937	-0.00042	2.87895
		Average	2.87894 ± 0.00005	
		Refraction correction	0.00015	
			<u>2.87909</u>	
Iodide Chromium (low non-metallics) (6.14×10^{-6})	13	2.87876	+0.00012	2.87888
	20	2.87902	± 0.00000	2.87902
	30	2.87909	-0.00018	2.87891
	40	2.87921	-0.00035	2.87886
	50	2.87945	-0.00053	2.87892
		Average	2.87892 ± 0.00007	
		Refraction correction	0.00015	
			<u>2.87907</u>	

DISCUSSION

1. Correction of Absorption

Using the equipment and procedures outlined above, X-ray films were taken of four different chromium samples, three films measured, and the lattice constants calculated. If smaller glancing angles in the front reflection region are used, then smaller lattice constants than the actual values are obtained, due to absorption. Consequently, in these cases it is necessary to make a correction for absorption in order to get the correct lattice constants. In the present investigation, a plot was made of lattice constants against different glancing angles, as shown in Figure 23. The relation between the lattice constant and angle of reflection was not linear, but was a curve, with the lattice constants changing rapidly at small angles, and remaining nearly horizontal from 75° to 90° . The curve shows that the constant, obtained by extrapolation to 90° , falls completely within the range of fluctuations of the constants, as calculated from the diffraction lines $(211) \alpha_1$ and α_2 . Therefore, there was no need for an absorption correction for the lattice calculated.

2. Calculation of Atomic Weight

Though the lattice constants of chromium samples could be obtained with great accuracy, without using any standard substance, the accuracy of the absolute value of these constants is still not known. The absolute value of the

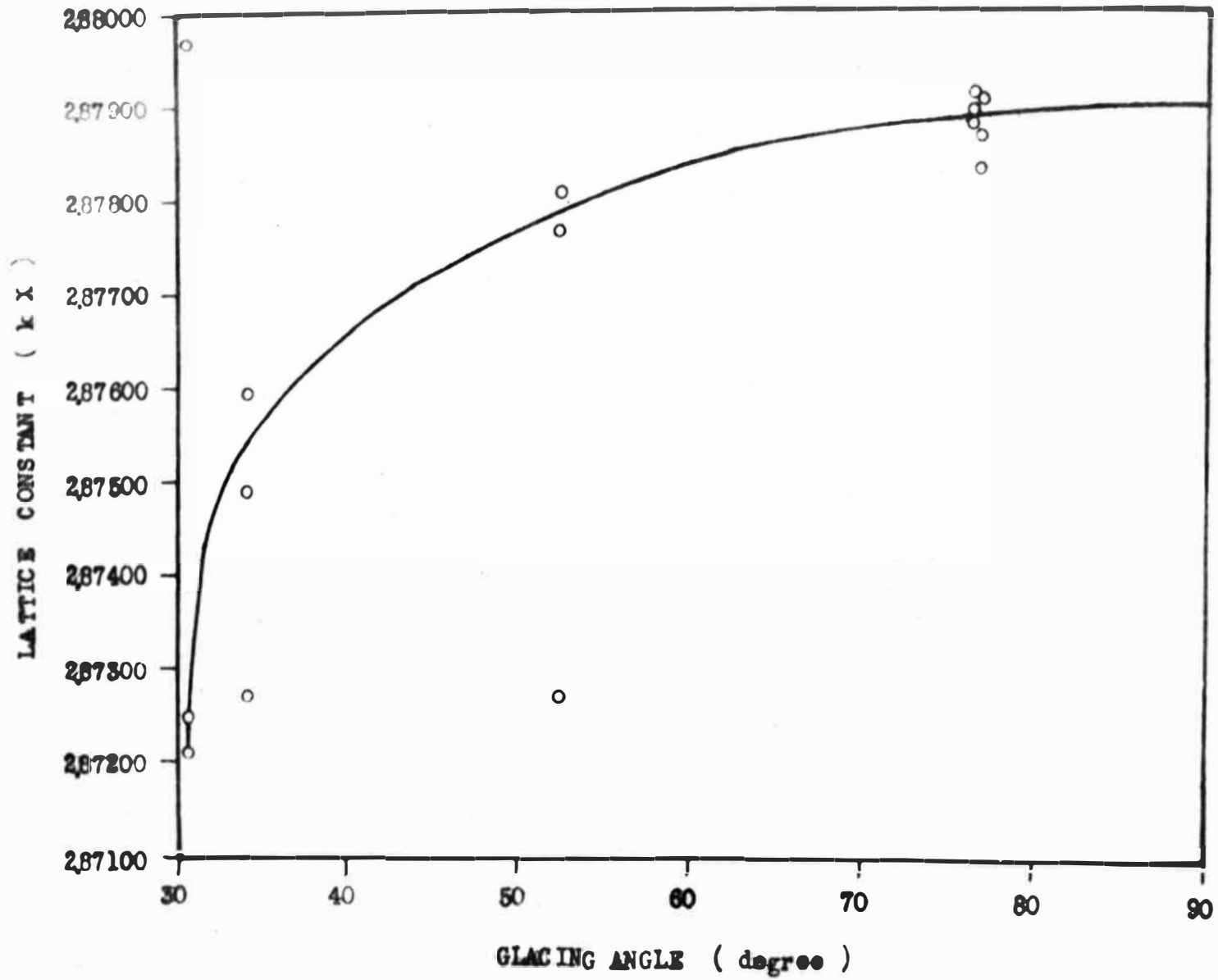


FIGURE 25. CHANGES OF LATTICE CONSTANTS AGAINST GLACING ANGLE DUE TO ABSORPTION

lattice constants can be tested by calculating the atomic weight, from the lattice constants obtained, and the density, of the respective substances. By comparing the resulting X-ray density atomic weight with its chemical weight, a conclusion concerning the precision of the X-ray method can be drawn. The atomic weight was calculated from the formula:

$$A_x = KN_s \frac{Vd}{N} \quad (16)$$

where A_x = X-ray atomic weight (g/mol)

K = 1.0002 (factor resulting from the correction of the molecular weight of calcite)

N_s = 6.0594×10^{23} (Siegbahn's Avogadro number)

V = Volume of the unit cell ($kx^3 \times 10^{-24}$)

d = Density (g/cc)

N = Number of atoms per unit cell.

Now, lattice constant of electrolytic chromium at $20^\circ = 2.87915$ kX, $d = 7.03$ g/cc, $N = 2$. Therefore,

$$A_x = 1.0002 \times 6.0594 \times 10^{23} \times (2.87915)^3 \times \frac{7.03}{2} = 50.63 \text{ g.}$$

The chemical atomic weight of chromium is 52.01 g. The difference between the two figures is probably due to the incorrect value for the specific gravity of chromium, concerning which until now no accurate data have been published. Otherwise, it would mean that there are vacancies in the chromium crystals. So the value of lattice constant of chromium can not be checked in this way, because of the insufficiently accurate density value.

3. Calculation of X-ray Density

The correct density of chromium, assuming that there are no imperfections in chromium crystals, can be calculated from the chemical atomic weight, and the precise lattice constant. For this X-ray density of chromium, the same equation (16) can be used:

$$d_x = \frac{AN}{KN_s V} \quad \dots \dots \dots (17)$$

where d_x = X-ray density (g/cc) at 20° C

A = The chemical atomic weight 52.01 g

N = 2

K = 1.0002

$N_s = 6.0594 \times 10^{23}$

$V = (2.87915 \text{ \AA})^3 \times 10^{-24}$ at 20° C

Therefore,
$$d = \frac{52.01 \times 2 \times 10^{24}}{1.0002 \times 6.0594 \times 10^{23} \times (2.87915)^3} =$$

7.1913 g/cc instead of 7.03 g/cc.

as obtained using rough density measurements.

SUMMARY

1. Each of four different pure chromium samples was thoroughly ground, placed in a quartz tube, the tube evacuated, then sealed, and the whole treated at 850° C for two and a half hours.
2. The fine powder in the heat treated sample, which would pass a 325 mesh screen, was used for the preparation of a sample for X-ray diffraction.
3. The powder patterns were indexed and a target of proper wave length selected, so that sharp diffraction lines with the largest possible glancing angles could be obtained. This radiation was that of chromium.
4. Next, the diffraction lines obtained were used to calculate the lattice constants of the sample.
5. Due to the very thin powder sample and large glancing angle, the absorption correction was neglected.
6. A refraction correction of 0.00015 kX was calculated and can be added to the final results if necessary (see Table XVI).
7. The lattice constants obtained at 20° C were $2.87914 \text{ kX} \pm 0.00005$ for electrolytic chromium, and $2.87908 \text{ kX} \pm 0.00007$ for iodide chromium (see Table XVI).
8. The average coefficients of expansion calculated ranged from 4.92×10^{-6} to 6.14×10^{-6} within the temperature range of 10° to 50° C (see Table XV).

9. The calculated atomic weight of chromium was 50.63 g., showing the incorrect density previously determined.
10. The X-ray density of chromium was 7.1913 g/cc at 20° C.

APPENDIX

Film Measurements. The individual line readings and lattice constant calculations from all films measured during experiments are recorded below. Cr- radiation is used. Two sets of lines in the front reflection, namely $(110)\alpha_1$, $(110)\beta$, and two sets of lines in the back reflection, namely $(211)\alpha_1$, $(211)\alpha_2$, are measured and $(211)\alpha_1$ is used to calculate the lattice constant of chromium.

1. Electrolytic Chromium

Film #788	Temperature 13° C			
	173.392 ± 143.335 = 316.727		316.729	30.057(ϕ)
	172.907 + 143.824 = 316.731			
Line read	96.550 + 20.509 = 117.059		117.066	
	92.748 + 24.325 = 117.073			
	Circumference		199.663	
F = 0.45076,	ϕ° = 13.548,	cos ϕ = 0.97217,		a = 2.87870

Film #789	Temperature 13° C			
	174.357 ± 144.192 = 318.549		318.544	30.165(ϕ)
	173.853 + 144.686 = 318.539			
Line read	97.283 + 21.188 = 118.471		118.478	
	93.487 + 24.997 = 118.484			
	Circumference		200.066	
F = 0.44985,	ϕ° = 13.570,	cos ϕ = 0.97208,		a = 2.87897

Film #790	Temperature 13° C			
	174.132 ± 143.984 = 318.116		318.113	30.148(ϕ)
	173.652 + 144.458 = 318.110			
Line read	97.129 + 20.979 = 118.108		118.113	
	93.307 + 24.812 = 118.119			
	Circumference		200.000	
F = 0.45000,	ϕ° = 13.567,	cos ϕ = 0.97210,		a = 2.87891

Film #791	Temperature 20° C			
	172.945 ± 142.775 = 315.720		315.719	30.170(ϕ)
	172.457 + 143.260 = 315.717			
Line read	95.918 + 19.824 = 115.742		115.745	
	92.098 + 23.649 = 115.747			
	Circumference		199.974	
F = 0.45006,	ϕ° = 13.578,	cos ϕ = 0.97205,		a = 2.87905

Film #792	Temperature 20° C			
	174.024 ± 143.857 = 317.881	317.881	30.167(φ)	
	173.562 + 144.319 = 317.881			
Line read	97.013 + 20.935 = 117.948	117.957		
	93.216 + 24.750 = 117.966			
	Circumference	199.924		
F = 0.45017,	φ° = 13.580,	Cos φ = 0.97204,	a = 2.87908	
Film #793	Temperature 20° C			
	174.100 ± 143.922 = 318.022	318.027	30.178(φ)	
	173.633 + 144.399 = 318.032			
Line read.	97.015 + 20.940 = 117.955	117.962		
	93.235 + 24.733 = 117.968			
	Circumference	200.065		
F = 0.44985,	φ° = 13.576,	Cos φ = 0.97206,	a = 2.87903	
Film #794	Temperature 30° C			
	173.715 ± 143.533 = 317.248	317.245	30.182	
	173.210 + 144.032 = 317.242			
Line read	96.668 + 20.601 = 117.269	117.279		
	92.870 + 24.419 = 117.289			
	Circumference	199.966		
F = 0.45008,	φ° = 13.584,	Cos φ = 0.97203,	a = 2.87911	
Film #795	Temperature 30° C			
	174.387 ± 144.232 = 318.619	318.614	30.155	
	173.879 + 144.730 = 318.609			
Line read	97.458 + 21.496 = 118.954	118.952		
	93.658 + 25.291 = 118.949			
	Circumference	199.662		
F = 0.45076,	φ° = 13.593,	Cos φ = 0.97199,	a = 2.87923	
Film #796	Temperature 30° C			
	174.634 ± 144.513 = 319.147	319.150	30.121	
	174.164 + 144.989 = 319.153			
Line read	97.773 + 21.901 = 119.674	119.674		
	93.976 + 25.697 = 119.673			
	Circumference	199.476		
F = 0.45118,	φ° = 13.590,	Cos φ = 0.97200,	a = 2.87920	
Film #797	Temperature 40° C			
	175.061 ± 144.840 = 319.901	319.906	30.221	
	174.577 + 145.333 = 319.910			
Line read	97.943 + 21.835 = 119.778	119.780		
	94.149 + 25.633 = 119.782			
	Circumference	200.126		
F = 0.44972,	φ° = 13.591,	Cos φ = 0.97200,	a = 2.87920	
Film #798	Temperature 40° C			
	170.584 ± 140.345 = 310.929	310.929	30.239	
	170.081 + 140.847 = 310.928			
Line read	93.503 + 17.416 = 110.919	110.921		
	89.709 + 21.213 = 110.922			
	Circumference	200.008		
F = 0.44998,	φ° = 13.607,	Cos φ = 0.97193,	a = 2.87941	

Film #799	Temperature 40° C			
	172.744 ± 142.604 = 315.348			
	172.276 + 143.079 = 315.355	315.352		30.140
Line read	95.836 + 19.937 = 115.773			
	92.061 + 23.726 = 115.787	115.780		
	Circumference		199.572	
F = 0.45097,	$\phi^{\circ} = 13.592,$	$\text{Cos } \phi = 0.97199,$		a = 2.87923

Film #800	Temperature 50° C			
	175.588 ± 145.438 = 321.026			
	175.127 + 145.897 = 321.024	321.025		30.150
Line read	98.682 + 22.712 = 121.394			
	94.989 + 26.512 = 121.410	121.402		
	Circumference		199.623	
F = 0.45085,	$\phi^{\circ} = 13.593,$	$\text{Cos } \phi = 0.97199,$		a = 2.87923

Film #801	Temperature 50° C			
	174.020 ± 143.803 = 317.823			
	173.538 + 144.295 = 317.833	317.828		30.217
Line read	97.067 + 21.167 = 118.234			
	93.273 + 24.957 = 118.230	118.232		
	Circumference		199.596	
F = 0.45091,	$\phi^{\circ} = 13.625,$	$\text{Cos } \phi = 0.97186,$		a = 2.87962

Film #802	Temperature 50° C			
	173.710 ± 143.507 = 317.217			
	173.229 + 143.995 = 317.224	317.221		30.203
Line read	96.772 + 20.860 = 117.632			
	92.985 + 24.657 = 117.642	117.637		
	Circumference		199.584	
F = 0.45094,	$\phi^{\circ} = 13.620,$	$\text{Cos } \phi = 0.97188,$		a = 2.87956

II. Sintered Electrolytic Chromium

Film #811	Temperature 10° C			
	174.460 ± 144.286 = 318.746			
	174.460 + 144.286 = 318.746	318.746		30.174
Line read	97.352 + 21.172 = 118.524			
	93.563 + 24.956 = 118.519	118.522		
	Circumference		200.224	
F = 0.44950,	$\phi^{\circ} = 13.563,$	$\text{Cos } \phi = 0.97211,$		a = 2.87888

Film #810	Temperature 10° C			
	174.710 ± 144.573 = 319.283			
	174.710 + 144.573 = 319.283	319.283		30.137
Line read	97.655 + 21.500 = 119.155			
	93.850 + 25.319 = 119.169	119.162		
	Circumference		200.121	
F = 0.44973,	$\phi^{\circ} = 13.554,$	$\text{Cos } \phi = 0.97215,$		a = 2.87876

Film #809	Temperature 10° C			
	175.743 ± 145.582 = 321.325			
	175.743 + 145.582 = 321.325	321.325		30.161
Line read	98.702 + 22.525 = 121.227			
	94.875 + 26.361 = 121.236	121.232		
	Circumference		200.093	
F = 0.44979,	$\phi^{\circ} = 13.566,$	$\text{Cos } \phi = 0.97210,$		a = 2.87891

Film #757	Temperature 11.7° C			
	171.042 ± 140.903 = 311.945			
	170.526 + 141.423 = 311.949	311.947		30.139
Line read	93.963 + 17.858 = 111.821			
	90.176 + 21.662 = 111.838	111.830		
	Circumference	200.117		
F = 0.44974,	$\phi^{\circ} = 13.555,$	$\text{Cos } \phi = 0.97215,$		a = 2.87876
Film #758	Temperature 11.7° C			
	172.785 ± 142.613 = 315.398			
	172.266 + 143.126 = 315.392	315.395		30.172
Line read	95.690 + 19.447 = 115.137			
	91.874 + 23.290 = 115.164	115.151		
	Circumference	200.244		
F = 0.44945,	$\phi^{\circ} = 13.561,$	$\text{Cos } \phi = 0.97212,$		a = 2.87885
Film #753	Temperature 13° C			
	175.664 ± 145.507 = 311.171			
	175.170 + 146.007 = 311.177	311.174		30.157
Line read	98.640 + 22.508 = 111.148			
	94.810 + 26.353 = 111.163	111.156		
	Circumference	200.018		
F = 0.44996,	$\phi^{\circ} = 13.569,$	$\text{Cos } \phi = 0.97209,$		a = 2.87894
Film #754	Temperature 13° C			
	173.187 ± 143.079 = 316.266			
	172.675 + 143.582 = 316.257	316.262		30.108
Line read	96.142 + 20.031 = 116.173			
	92.340 + 23.857 = 116.197	116.185		
	Circumference	200.077		
F = 0.44983,	$\phi^{\circ} = 13.543,$	$\text{Cos } \phi = 0.97219,$		a = 2.87864
Film #755	Temperature 13° C			
	171.695 ± 141.574 = 313.269			
	171.191 + 142.084 = 313.275	313.272		30.121
Line read	94.703 + 18.558 = 113.261			
	90.905 + 22.371 = 113.276	113.269		
	Circumference	200.003		
F = 0.44999,	$\phi^{\circ} = 13.554,$	$\text{Cos } \phi = 0.97215,$		a = 2.87876
Film #759	Temperature 20° C			
	173.620 ± 143.432 = 317.052			
	173.095 + 143.952 = 317.047	317.050		30.188
Line read	96.584 + 20.496 = 117.080			
	92.776 + 24.320 = 117.096	117.088		
	Circumference	199.962		
F = 0.45009,	$\phi^{\circ} = 13.587,$	$\text{Cos } \phi = 0.97201,$		a = 2.87917
Film #760	Temperature 20° C			
	173.407 ± 143.274 = 316.681			
	172.926 + 143.761 = 316.687	316.684		30.133
Line read	96.365 + 20.231 = 116.596			
	92.564 + 24.051 = 116.615	116.602		
	Circumference	200.082		
F = 0.44982,	$\phi^{\circ} = 13.554,$	$\text{Cos } \phi = 0.97215,$		a = 2.87876

Film #761	Temperature 20° C				
	173.605 ±	143.431 =	317.036		
	173.090 +	143.946 =	317.036	317.036	30.174
Line read	96.534 +	20.459 =	116.993		
	92.740 +	24.270 =	117.010	117.002	
	Circumference			200.034	
F = 0.44992,	ϕ° = 13.576,	Cos ϕ = 0.97206,	a = 2.87903		
Film #765	Temperature 30° C				
	173.847 ±	143.670 =	317.517		
	173.330 +	144.180 =	317.510	317.514	30.177
Line read	96.863 +	20.805 =	117.668		
	93.080 +	24.595 =	117.675	117.672	
	Circumference			199.842	
F = 0.45036,	ϕ° = 13.591,	Cos ϕ = 0.97200,	a = 87920		
Film #766	Temperature 30° C				
	174.031 ±	143.887 =	317.918		
	173.517 +	144.404 =	317.921	317.920	30.144
Line read	97.084 +	21.087 =	118.171		
	93.275 +	24.910 =	118.185	118.178	
	Circumference			199.742	
F = 0.45058,	ϕ° = 13.582,	Cos ϕ = 0.97203,	a = 2.87911		
Film #767	Temperature 30° C				
	173.862 ±	143.710 =	317.572		
	173.353 +	144.210 =	317.563	317.567	30.152
Line read	96.873 +	20.852 =	117.725		
	93.055 +	24.685 =	117.740	117.733	
	Circumference			199.834	
F = 0.45037,	ϕ° = 13.580,	Cos ϕ = 0.97204,	a = 2.87908		
Film #762	Temperature 40° C				
	174.935 ±	144.705 =	319.640		
	174.434 +	145.215 =	319.649	319.645	30.230
Line read	97.800 +	21.765 =	119.565		
	93.990 +	25.595 =	119.585	119.575	
	Circumference			200.070	
F = 0.44984,	ϕ° = 13.599,	Cos ϕ = 0.97197,	a = 2.87929		
Film #763	Temperature 40° C				
	171.659 ±	141.473 =	313.132		
	171.180 +	141.956 =	313.136	313.134	30.186
Line read	94.553 +	18.417 =	112.970		
	90.756 +	22.234 =	112.990	112.980	
	Circumference			200.154	
F = 0.44965,	ϕ° = 13.573,	Cos ϕ = 0.97207,	a = 2.87901		
Film #764	Temperature 40° C				
	171.888 ±	141.672 =	313.560		
	171.400 +	142.165 =	313.565	313.563	30.216
Line read	94.745 +	18.665 =	113.410		
	90.932 +	22.483 =	113.415	113.413	
	Circumference			200.150	
F = 0.44966,	ϕ° = 13.587,	Cos ϕ = 0.97201,	a = 2.87917		

Film #768	Temperature 50° C			
	173.608 ± 143.445 = 317.053			
	173.110 + 143.935 = 317.045	317.049		30.163
Line read	96.725 + 20.775 = 117.500			
	92.915 + 24.610 = 117.525	117.513		
	Circumference	199.536		
F = 0.45105,	$\phi^{\circ} = 13.605,$	$\text{Cos } \phi = 0.97194,$		$a = 2.87938$

Film #769	Temperature 50° C			
	173.327 ± 143.192 = 316.519			
	172.792 + 143.718 = 316.510	316.515		30.135
Line read	96.514 + 20.712 = 117.226			
	92.731 + 24.502 = 117.233	117.230		
	Circumference	199.285		
F = 0.45161,	$\phi^{\circ} = 13.609,$	$\text{Cos } \phi = 0.97192,$		$a = 2.87944$

Film #770	Temperature 50° C			
	172.685 ± 142.565 = 315.250			
	172.200 + 143.058 = 315.258	315.254		30.120
Line read	95.840 + 20.034 = 115.874			
	92.042 + 23.852 = 115.894	115.884		
	Circumference	199.370		
F = 0.45142,	$\phi^{\circ} = 13.597,$	$\text{Cos } \phi = 0.97197,$		$a = 2.87929$

IV. Iodide Chromium (Low Non-Metallic)

Film #787	Temperature 13° C			
	173.338 ± 143.303 = 316.641			
	172.862 + 143.789 = 316.651	316.646		30.035
Line read	96.488 + 20.684 = 117.172			
	92.688 + 24.490 = 117.178	117.175		
	Circumference	199.471		
F = 0.45119,	$\phi^{\circ} = 13.551,$	$\text{Cos } \phi = 0.97216,$		$a = 2.87873$

Film #786	Temperature 13° C			
	176.356 ± 146.312 = 322.668			
	175.883 + 146.793 = 322.676	322.672		30.044
Line read	99.525 + 23.619 = 123.144			
	95.761 + 27.403 = 123.164	123.154		
	Circumference	199.518		
F = 0.45109,	$\phi^{\circ} = 13.553,$	$\text{Cos } \phi = 0.97215,$		$a = 2.87876$

Film #785	Temperature 13° C			
	173.972 ± 143.910 = 317.882			
	173.506 + 144.384 = 317.890	317.886		30.062
Line read	97.122 + 21.169 = 118.291			
	93.342 + 24.968 = 118.310	118.301		
	Circumference	199.585		
F = 0.45094,	$\phi^{\circ} = 13.556,$	$\text{Cos } \phi = 0.97214,$		$a = 2.87879$

Film #783	Temperature 20° C				
	175.046 ±	144.941 =	319.987	319.986	30.105
	174.584 +	145.400 =	319.984		
Line read	98.145 +	22.262 =	120.407	120.412	
	94.352 +	26.064 =	120.416		
	Circumference			199.574	
F = 0.45096,	$\phi^{\circ} = 13.576,$	$\text{Cos } \phi = 0.97206,$			a = 2.87903
Film #782	Temperature 20° C				
	175.684 ±	145.532 =	321.216	321.219	30.152
	175.189 +	146.032 =	321.221		
Line read	98.674 +	22.697 =	121.371	121.378	
	94.865 +	26.520 =	121.385		
	Circumference			199.841	
F = 0.45036,	$\phi^{\circ} = 13.579,$	$\text{Cos } \phi = 0.97205,$			a = 2.87905
Film #781	Temperature 20° C				
	174.925 ±	144.706 =	319.531	319.527	30.119
	174.321 +	145.202 =	319.523		
Line read	97.870 +	21.900 =	119.770	119.776	
	94.054 +	25.728 =	119.782		
	Circumference			199.751	
F = 0.45056,	$\phi^{\circ} = 13.570,$	$\text{Cos } \phi = 0.97208,$			a = 2.87897
Film #780	Temperature 30° C				
	173.728 ±	143.613 =	317.341	317.343	30.115
	173.245 +	144.100 =	317.345		
Line read	96.809 +	20.905 =	117.714	117.715	
	93.016 +	24.700 =	117.716		
	Circumference			199.628	
F = 0.45084,	$\phi^{\circ} = 13.577,$	$\text{Cos } \phi = 0.97206,$			a = 2.87903
Film #779	Temperature 30° C				
	173.688 ±	143.552 =	317.240	317.245	30.136
	173.236 +	144.014 =	317.250		
Line read	96.763 +	20.875 =	117.638	117.636	
	92.970 +	24.664 =	117.634		
	Circumference			199.609	
F = 0.45088,	$\phi^{\circ} = 13.588,$	$\text{Cos } \phi = 0.97201,$			a = 2.87917
Film #778	Temperature 30° C				
	173.775 ±	143.668 =	317.343	317.347	30.107
	173.320 +	144.130 =	317.450		
Line read	96.841 +	20.980 =	117.821	117.831	
	93.074 +	24.766 =	117.840		
	Circumference			199.516	
F = 0.45109,	$\phi^{\circ} = 13.581,$	$\text{Cos } \phi = 0.97204,$			a = 2.87908
Film #777	Temperature 40° C				
	174.765 ±	144.622 =	319.387	319.392	30.143
	174.310 +	145.086 =	319.396		
Line read	97.853 +	21.962 =	119.815	119.820	
	94.070 +	25.755 =	119.825		
	Circumference			199.572	
F = 0.45097,	$\phi^{\circ} = 13.594,$	$\text{Cos } \phi = 0.97199,$			a = 2.87923

Film #776	Temperature 40° C				
	171.461 ±	141.324 =	312.785	312.787	30.137
	171.000 +	141.788 =	312.788		
Line read	94.573 +	18.649 =	113.222	113.227	
	90.770 +	22.462 =	113.232		
		Circumference	199.560		
F = 0.45099,	$\phi^{\circ} = 13.591,$	$\cos \phi = 0.97200,$			$a = 2.87920$
Film #775	Temperature 40° C				
	174.095 ±	143.949 =	318.044	318.050	30.146
	173.591 +	144.464 =	318.055		
Line read	97.175 +	21.223 =	118.398	118.400	
	93.370 +	25.032 =	118.402		
		Circumference	199.650		
F = 0.45079,	$\phi^{\circ} = 13.590,$	$\cos \phi = 0.97200,$			$a = 2.87920$
Film #774	Temperature 50° C				
	175.025 ±	144.879 =	319.904	319.902	30.146
	174.518 +	145.382 =	319.900		
Line read	98.150 +	22.314 =	120.464	120.472	
	94.346 +	26.134 =	120.480		
		Circumference	199.430		
F = 0.45129,	$\phi^{\circ} = 13.605,$	$\cos \phi = 0.97194,$			$a = 2.87938$
Film #773	Temperature 50° C				
	172.828 ±	142.655 =	315.483	315.483	30.173
	172.324 +	143.158 =	315.482		
Line read	95.913 +	20.083 =	116.001	115.996	
	92.096 +	23.895 =	115.991		
		Circumference	199.487		
F = 0.45116,	$\phi^{\circ} = 13.613,$	$\cos \phi = 0.97191,$			$a = 2.87947$
Film #772	Temperature 50° C				
	172.799 ±	142.611 =	315.410	315.415	30.188
	172.353 +	143.067 =	315.420		
Line read	95.868 +	20.011 =	115.879	115.873	
	92.068 +	23.798 =	115.866		
		Circumference	199.542		
F = 0.45103,	$\phi^{\circ} = 13.616,$	$\cos \phi = 0.97190,$			$a = 2.87950$

BIBLIOGRAPHY

1. Barrett, G. S., Structure of Metals, McGraw-Hill, New York, 150 pp., 1952.
2. Chevenard, P., Comptes rend., p. 174, 109, 1922.
3. Disch, J., Z. Physik, p. 5, 173, 1921.
4. Fine, M. E., J. of Metals Tran., AIME, p. 189, 56, 1951.
5. Hidnert, P., J. of Research of the National Bureau of Standards, p. 26, 81, 1941.
6. Hull, A. W., Phy. Rev., p. 14, 540, 1919.
7. Laue, M., Ann. Physik, p. 41, 971, 1913.
8. MacNair, D., Rev. of Scientific Instruments, p. 12, 66, 1941.
9. Straumanis, M., Zeit Krist, p. 104, 167, 1942.
10. Straumanis, M., Am. Mineralogist, p. 37, 48, 1952.
11. Straumanis, M., Anorg. Chem., p. 238, 175, 1938.
12. Wein, W., Handb. d. Experimental-Phys., p. 24, 94, 1930.
13. Westgren, A., J. Iron and Steel Institute, p. 117, 383, 1928.



82677

VITA

The author was born on October 5, 1918, in Peiping, Hopei, China. He received the degree of Bachelor of Science in Mining and Metallurgical Engineering in 1941 from Chiao-Tung University, China. After graduation, he worked in the Tze-Yui and Tze-Shu Steel Works of the National Resources Commission of China from 1941 to 1946, in the Iron and Steel Division of the same Commission from 1946 to 1948 and in the Taiwan Steel Works of the same Commission from 1948 to 1951. He came to the United States of America in January 1952 and enrolled as a graduate student in the Metallurgical Engineering Department of the Missouri School of Mines and Metallurgy of the University of Missouri, Rolla, Missouri.